Progression of Autoimmune Hepatitis is Mediated by IL-18-Producing Dendritic Cells and Hepatic CXCL9 Expression in Mice

Aki Ikeda[1,2,#], Nobuhiro Aoki[1,2,#], Masahiro Kido[1,2,#], Satoru Iwamoto[1,2], Hisayo Nishiura[1,2], Ryutaro Maruoka[1,2], Tsutomu Chiba[2], and Norihiko Watanabe[1,2,*]

[1]Center for Innovation in Immunoregulative Technology and Therapeutics, and [2]Department of Gastroenterology and Hepatology, Graduate School of Medicine, Kyoto University, Kyoto 606-8501, Japan

[#] These authors contributed equally to this work.

Keywords: autoimmune hepatitis; fatal progression; IL-18; dendritic cell; CXCR3-CXCL9 axis

* *Correspondence: Norihiko Watanabe, Address: Yoshidakonoe-cho Sakyo-ku Kyoto city, Kyoto 606-8501, Japan, E-mail: norihiko@kuhp.kyoto-u.ac.jp, Tel:+81-75-751-4319, Fax:+81-75-751-4303*

Abbreviations: AIH, autoimmune hepatitis; ANA, anti-nuclear antibody; DCs, dendritic cells; GC, germinal center; ICOS, inducible costimulator; IL-21R, IL-21 receptor; NTx, neonatal thymectomy; NTx–PD-1$^{-/-}$ mice, PD-1–deficient BALB/c mice thymectomized three days after birth; PD-1, programmed cell death 1; PNA, peanut agglutinin; $T_{FH,}$ follicular helper T; Tregs, regulatory T cells

Acknowledgements: We thank Dr. Taku Okazaki and Tasuku Honjo for providing of PD-1 deficient mice; Dr. Dovie Wylie for assistance in preparation of the manuscript; Ms. Chigusa Tanaka for excellent technical assistance; Drs. Shuh Narumiya, Nagahiro Minato, Shimon Sakaguchi, Takeshi Watanabe and Ichiro Aramori for critical discussion and suggestions.

Author Contributions: A.I., N.A., M.K. and N.W. designed experiments. A.I., N.A., M.K., S.I., H.N., R.M. and N.W. performed experiments. A.I., N.A. M.K., and N.W. analyzed data. A.I., N.A. and N.W. wrote the manuscript. T.C. critically revised the manuscript for important intellectual content. N.W. initiated and directed the study.

Potential conflict of interest: Nothing to report.

Financial support: The Center for Innovation in Immunoregulative Technology and Therapeutics is supported in part by the Special Coordination Funds for Promoting Science and Technology of the Japanese Government and in part by Astellas Pharma Inc. in the Formation of Innovation Center for Fusion of Advanced Technologies Program. This work is partially supported by Grants-in-aid for Scientific Research 20390207, 21229009, 23590973 from Japan Society for the Promotion of Science (JSPS), a Health and Labour Sciences Research Grant for Research on Intractable Diseases, and Research on Hepatitis from the Ministry of Health, Labour and Welfare, Japan, Grants-in-Aid for Research by The Kato Memorial Trust for Nambyo Research, and The Waksman Foundation of Japan.

Abstract

Clinical manifestations of autoimmune hepatitis (AIH) range from mild chronic to acute, sometimes fulminant hepatitis. However, it is unknown how the progression to fatal hepatitis occurs. We developed a mouse model of fatal AIH by inducing a concurrent loss of Foxp3$^+$ regulatory T cells and PD-1–mediated signaling. In this model, dysregulated follicular helper T cells in the spleen are responsible for the induction, and the CCR6-CCL20 axis is crucial for the migration of these T cells into the liver. Using this fatal AIH model, we aimed to clarify key molecules triggering fatal AIH progression. During progression, T-bet together with IFN-γ and CXCR3 were highly expressed in the inflamed liver, suggesting Th1-type inflammation. T cells that dominantly expanded in the spleen and the inflamed liver were CXCR3-expressing CD8$^+$ T cells; depletion of these CD8$^+$ T cells suppressed AIH progression. Expression of one CXCR3 ligand, CXCL9, was elevated in the liver. CXCL9 expressing macrophages/Kupffer cells were co-localized with infiltrating T cells, and *in vivo* administration of anti-CXCL9 suppressed AIH progression. In addition, serum levels of IL-18 but not IL-1β were elevated during progression, and dendritic cells in the spleen and liver highly produced IL-18. *In vivo* administration of anti-IL-18R suppressed the increase of splenic CXCR3$^+$ T cells and the progression to fatal AIH. Moreover, TNF-α but not IFN-γ was involved in upregulating CXCL9 in the liver and for increased serum levels of IL-18. *Conclusion:* These data suggest that in our mouse model, fatal progression of AIH is mediated by IL-18-dependent differentiation of T cells into Th1 cells and effector T cells, respectively, and that CXCR3-CXCL9 axis-dependent migration of those T cells is crucial for fatal progression.

Human autoimmune hepatitis (AIH) typically presents as asymptomatic or mild chronic hepatitis. However, presentation as acute severe hepatitis also occurs, and some of these AIH patients manifest liver failure at initial presentation.[1,2] Untreated patients with severe AIH rapidly decline, with a mortality rate of up to 50% from 3 to 5 years following diagnosis.[3] Patients progressing to acute liver failure respond poorly to corticosteroid treatment, some of them needing liver transplantation.[4, 5] In addition, approximately 20 to 30% of patients undergoing liver transplantation for AIH develop features of recurrent disease; in some, recurrent AIH behaves more aggressively, with progression to cirrhosis and graft failure.[6] However, it is unknown how this progression to fatal hepatic damages occurs.

Recently, we developed a mouse model of spontaneous fatal AIH.[7-11] Neither *programmed cell death 1*-deficient mice *(PD-1*$^{-/-}$ mice) nor BALB/c mice thymectomized three days after birth (NTx mice) developed any inflammation of the liver. In *PD-1*$^{-/-}$ BALB/c mice with neonatal thymectomy (NTx–*PD-1*$^{-/-}$ mice), however, immune dysregulation by a concurrent loss of naturally arising Foxp3^{+} regulatory T cells (Tregs) and PD-1-mediated signaling induced fatal AIH. Massive destruction of the parenchyma of the liver resulted in most mice dying by four weeks. Fatal AIH in NTx–*PD-1*$^{-/-}$ mice was characterized by CD4^{+} and CD8^{+} T-cell infiltration with massive lobular necrosis in the liver and by hyper-gammaglobulinemia and production of anti-nuclear antibodies (ANA).[7, 8]

In our mouse model of fatal AIH, we identified induction sites, responsible T cell subsets, and key molecules for induction of AIH.[8] The spleen is an induction site for fatal AIH, and splenic CD4^{+} T cells were autonomously differentiated into follicular helper T (T_{FH}) cells in two-week-old NTx–*PD-1*$^{-/-}$ mice. T_{FH} cells expressing Bcl6, interleukin (IL)-21, IL-21 receptor, inducible costimulator (ICOS), and CXCR5 comprise a newly defined effector T cell subset that powerfully assists B cells in forming germinal centers (GCs).[12] Indeed, in NTx–*PD-1*$^{-/-}$ mice, the dysregulated T_{FH} cells promoted hyper-gammaglobulinemia and ANA production. In addition, these T_{FH} cells in the spleen directly migrated into the liver via the CCR6-CCL20 axis, triggering induction of fatal AIH.[8]

On the other hand, in the progression phase of AIH in three-week-old NTx–*PD-1*$^{-/-}$ mice, infiltrated CD4^{+} and CD8^{+} T cells in the liver produced large amounts of

inflammatory cytokines, such as IFN-γ and TNF-α.[7, 8] Therefore, dysregulated T_{FH} cells in the induction and Th1 cells with effector $CD8^+$ T cells in the progression may play their roles at different time points in the development of fatal AIH. In this study, using our mouse model, we examined mechanisms in the progression process to identify key molecules triggering fatal AIH progression. We found that in the progression, CXCR3-expressing Th1 cells and $CD8^+$ effector T cells infiltrated in the liver, $CD8^+$ effector T cells triggering the fatal destruction of the liver; that hepatic macrophages/Kupffer cells producing CXCL9 is critical for migration of these T cells; and that DC-derived IL-18 is critical for differentiation of Th1 cells and $CD8^+$ effector T cells. These data suggest that in this mouse model of AIH, IL-18 and the CXCR3-CXCL9 axis are critical for T-cell differentiation and migration in fatal progression of AIH.

Materials and Methods

BALB/c mice were purchased from Japan SLC (Shizuoka, Japan), and *PD-1*$^{-/-}$ on a BALB/c background were generated as described previously.[13] These mice were bred and housed under specific pathogen-free conditions. Thymectomies were performed as described.[7-11] All mouse protocols were approved by the Institute of Laboratory Animals, Graduate School of Medicine, Kyoto University.

All other protocols for histological and immunohistological analysis, real-time quantitative reverse-transcription polymerase chain reactions (RT-PCR), flow cytometry analysis and isolation of single cells, administration of Abs *in vivo*, enzyme-linked immunosorbent assay (ELISA), *in vivo* injection of cytokines, DC coculture, and statistical analysis are detailed in the supplemental materials and methods.

Results

T-bet, IFN-γ, and CXCR3 Are Highly Upregulated in Inflamed Livers of Three-Week-Old NTx-PD-1$^{-/-}$ Mice. In our mouse model, AIH induction was started as early as two weeks of age by dysregulated T_{FH} cells in the spleen.[7, 8] As shown in Fig. 1A, livers in two-week-old NTx–*PD-1*$^{-/-}$ mice showed mononuclear cell infiltrations, predominantly in the portal area, as described.[7] Within seven days of induction, these mononuclear cell infiltrations rapidly progressed and were followed by massive destruction of the parenchyma of the liver (Fig. 1A). To investigate whether cytokines contributed to the severely inflamed livers of these three-week-old NTx–*PD-1*$^{-/-}$ mice, we performed real-time quantitative RT-PCR analysis to measure the expression levels of mRNA encoding T cell lineage-specific transcription factors and various related cytokines. In contrast to expression of Th2 or Th17-related molecules, expression of Th1 lineage-specific transcription factor T-bet, together with IFN-γ and TNF-α, were upregulated in inflamed liver tissues of these mice (Fig. 1B). These data suggest that inflammatory cytokines related to Th1-type inflammation may be involved in the fatal progression of AIH. Notably, we found that in the inflamed livers of these mice, mRNA expressions of CXCR3 were highly upregulated along with Th1-related molecules (Fig. 1C). Although AIH induction was mediated by dysregulated T_{FH} cells in the spleen, in the progression phase of AIH, Th1-type responses were predominant.

T Cells Dominantly Expanded in the Inflamed Liver Were CXCR3-Expressing CD8$^+$ T Cells. Next, we monitored T cell numbers of the liver, spleen, and mesenteric lymph nodes in NTx–*PD-1*$^{-/-}$ mice from 1 to 3 weeks old (Fig. 1D). In the AIH progression phase in three-week-old mice, we found that $CD8^+$ T cells, and to a lesser extent $CD4^+$ T cells, extensively increased in the liver, as described previously.[7] Notably, the predominant increase of $CD8^+$ T cells at three weeks was observed only in the liver but not in the spleen or mesenteric lymph nodes (Fig. 1D), implying that $CD8^+$ T cells had accumulated in the severely inflamed liver. In addition, we analyzed splenic and hepatic $CD8^+$ T-cell expression of the chemokine receptors CCR6, CCR9, and CXCR3 by flow cytometry. As with $CD4^+$ T cells in the spleen and liver,[8] splenic and hepatic $CD8^+$ T cells mainly expressed CXCR3 in three-week-old NTx–*PD-1*$^{-/-}$ mice (Fig. 1E).

CD8$^+$ T Cells During the Progression of AIH Were Indispensable for Fatal Destruction of the Liver. In a previous study, we showed that in the induction of fatal AIH, CD4$^+$ T cells are indispensable for recruiting CD8$^+$ T cells in the liver and that CD8$^+$ T cells may be major effector T cells, fatally destroying the liver in AIH progression.[8] To examine whether depletion of CD8$^+$ T cells in the progression is sufficient to suppress fatal liver destruction, AIH-developed NTx–*PD-1*$^{-/-}$ mice were injected intraperitoneally at fourteen days after NTx and then once a week with anti-CD8 mAbs *in vivo* (Fig. 2A). After two injections of anti-CD8, the number of CD8$^+$ T cells in the spleen was greatly reduced (Fig. 2B). Although depleting CD8$^+$ T cells did not completely suppress hepatic infiltrations of mononuclear cells, the infiltration of CD4$^+$ and CD8$^+$ T cells was diminished, and fatal progression of AIH was suppressed by the treatment (Fig. 2C-2E). These data suggest that CXCR3-expressing CD8$^+$ T cells extensively infiltrating the liver are indispensable for fatal progression.

Production of a CXCR3 Ligand, CXCL9, Was Elevated in the Fatal Progression of AIH. CXCR3-expressing T cells can be guided by three ligands — CXCL9/MIG, CXCL10/IP-10, and CXCL11/I-TAC — and expression of these CXCR3 ligands in the inflamed tissues determines inflamed-tissue–specific infiltration of CXCR3-expressing T cells in various immunoinflammatory settings, including autoimmune diseases.[14-17] We performed real-time quantitative RT-PCR analysis to measure the expression levels of mRNA encoding these three CXCR3 ligands. In contrast to non-inflamed livers in the control mice, severely inflamed livers of 3-week-old NTx–*PD-1*$^{-/-}$ mice showed markedly elevated gene expression of CXCL9 but not of CXCL10 and CXCL11 (Fig. 3A). In contrast to inflamed livers, no organs except those with inflamed gastric tissues showed a significantly increased level of mRNA expression of CXCL9 (Fig. 3B).

In addition, we confirmed elevated protein expression of CXCL9 only in the inflamed liver but not the stomach by immunohistochemistry (Fig. 3C and supplementary Fig. 1). Furthermore, when we looked at serum concentrations of CXCL9 and CXCL10 at one to four weeks of age, the serum level of CXCL9 but not CXCL10, at three to four weeks of age, was significantly higher than controls (Fig. 3D). These data suggest that CXCL9 plays a key role in the progression of AIH.

In Fatal Progression of AIH, the CXCR3-CXCL9 Axis Was Crucial for T-cell

Migration into the Liver. To determine whether the axis formed by CXCR3 and its ligands contributes to T-cell migration leading to fatal progression of AIH, NTx–*PD-1*$^{-/-}$ mice were injected intraperitoneally at one day after NTx and then once a week with anti-CXCL9 and/or anti-CXCL10 mAbs *in vivo*. After four injections, in contrast to anti-CXCL10 injections, anti-CXCL9 injections induced a significantly higher survival rate (Fig. 4A and 4B). Administering anti-CXCL9 and a combination with anti-CXCL9 and anti-CXCL10, but not anti-CXCL10 alone, greatly reduced infiltration of $CD4^+$ and $CD8^+$ T cells into the liver and liver destruction at four weeks (Fig. 4C). These data suggest that in the progression phase of fatal AIH, the CXCR3-CXCL9 axis is crucial for migration of Th1 cells and effector $CD8^+$ T cells into the liver.

The Main Cellular Source of CXCL9 Was Hepatic Macrophages/Kupffer Cells in the Progression of AIH. Next, we examined which cell types express CXCL9 in the inflamed liver by immunohistochemistry. We found that the majority of CXCL9-expressing cells in the inflamed liver were F4/80 antigen positive macrophages/Kupffer cells and that $CD4^+$ and $CD8^+$ T cells were co-localized with CXCL9-expressing cells in the inflamed liver (Fig. 5A).

In AIH progression, mRNA expression of IFN-γ and TNF-α in the inflamed liver as well as serum levels of these cytokines were markedly elevated[7-10], and IFN-γ mediated the induction of all three CXCR3 ligands: CXCL9, CXCL10, and CXCL11. [14, 15] When we injected intraperitoneally with 10 mg/kg of IFN-γ and TNF-α in four-week-old *PD-1*$^{-/-}$ mice, after two hours, IFN-γ and TNF-α significantly upregulated mRNA expression of both CXCL9 and CXCL10 in the liver. Interestingly, we found sustained CXCL9 upregulation by TNF-α (Fig. 5B). Indeed, neutralization of TNF-α but not IFN-γ suppressed hepatic CXCL9-expression in four-week-old NTx–*PD-1*$^{-/-}$ mice (Fig. 5C).

In NTx–*PD-1*$^{-/-}$ mice, TNF-α is essential in the induction of AIH by upregulating hepatic CCL20 expression, allowing TNF-α–producing activated T cells to migrate from the spleen into the liver.[10] In AIH progression, immunohistochemistry for TNF-α revealed TNF-α production in several infiltrating cell types (Fig. 5D, left panels), suggesting that TNF-α–dependent upregulation of CXCL9 expression may be induced by hepatic macrophages/Kupffer cells in autocrine fashion and/or by activated T cells in paracrine fashion. However, after migration of TNF-α–producing activated T cells into

the liver, neutralizing serum levels of TNF-α could not suppress CXCL9 expression in the liver and serum levels of CXCL9 (Fig. 5D right panels and 5E). These data suggest that TNF-α secretion in autocrine and/or paracrine fashion may induce uncontrollable CXCL9 expression in the progression of AIH, resulting in unsuccessful anti-TNFα monotherapy as described.[10]

Serum Levels of IL-18 Were Elevated in AIH Progression, and In Vivo Administration of Blocking Abs for IL-18R Signaling Suppressed the Development of Fatal AIH. IL-12 is decisive in the development of Th1 subsets. A recent study showed that IL-12 can trigger naïve T cells to transitionally differentiate into T cells with features of T_{FH} and Th1 cells, [18, 19] However, neutralizaing IL-12p40 did not suppress hepatic inflammation as described previously[8] (supplementary Fig. 2). In addition, although IFN-γ has been shown to be essential for IL-12 induced Th1 differentiation,[20] neutralizing it did not suppress the development of AIH.[9] These data suggest that IL-12 is not exclusively involved in differentiation into T cells with features of Th1 cells in the progression of fatal AIH.

Serum levels of IL-18 are increased in patients with AIH and fatal hepatitis.[21, 22] IL-18 is critical for liver injury in mice sequentially treated with *P. acnes* and LPS, and for acute hepatic injury induced by concanavalin A (Con A).[23, 24] When we looked at serum levels of IL-18 at one to three weeks of age, those of IL-18 but not IL-1β were elevated, and IL-18 elevation gradually increased through the progression of AIH (Fig. 6A and 6B). IL-18 signals through the IL-18 receptor complex (IL-18R), and IL-18R contains the heterodimer IL-18Rα and IL-18Rβ subunits. The IL-18Rα subunit is responsible for extracellular binding of IL-18, whereas the IL-18Rβ subunit is nonbinding but confers high affinity binding for the ligand and is responsible for biological signals. [25, 26] Therefore, to examine the roles of IL-18 in AIH development, NTx–*PD-1*$^{-/-}$ mice at one day after thymectomy were injected with IL-18Rβ mAb, which can neutralize the IL-18–mediating biological function in IL-18R–expressing cells. Administering anti-IL-18Rβ but not anti-IL-1β suppressed mononuclear cell infiltration, including $CD4^+$ and $CD8^+$ T cells, in the liver (Fig. 6C and 6D), resulting in decreased serum concentrations of aspartate aminotransferase and alanine aminotransferase and a significantly increased survival rate at four weeks of age (Fig. 6E and 6F). These data indicate that IL-18–mediated signaling is critical for the development of fatal AIH in

NTx–*PD-1*$^{-/-}$ mice.

IL-18 Is Mainly Produced by DCs in the Spleen and Liver of NTx–PD-1*$^{-/-}$ *Mice. Next, we investigated how IL-18 mediates fatal AIH progression in NTx–*PD-1*$^{-/-}$ mice. We isolated mononuclear cells from the liver and spleen of 2.5-week-old NTx–*PD-1*$^{-/-}$ mice, and purified them to $CD3^+CD4^+$ T cells, $CD3^+CD8^+$ T cells, $B220^+$ B cells, $CD11b^+CD11c^-$ macrophages, $CD11c^+$ DCs, and $CD3^-DX5^+$ NK cells, then measuring mRNA expression of IL-18. We found that isolated splenic and hepatic DCs increased IL-18 mRNA expression, together with upregulated expression of NACHT, LRR, and pyrin domain-containing ptotein-3 (NALP3) and, to a lesser extent, IL-1β (Fig. 7A and 7B). In contrast, when we cultured isolated splenic DCs, IL-18 but not IL-1β was secreted from DCs from NTx–*PD-1*$^{-/-}$ mice but not from *PD-1*$^{-/-}$ mice (Fig. 7C and data not shown). These data suggest that in NTx–*PD-1*$^{-/-}$ mice, DCs non-canonically secrete IL-18 by activating inflammasome and promoting further differentiation of $CD4^+$ T cells into Th1 cells and $CD8^+$ T cells into effector T cells, respectively.

DCs as well as CD4*$^+$ *and CD8*$^+$ *T Cells in the Spleen and Liver Expressed IL-18R in NTx–PD-1*$^{-/-}$ *Mice. To evaluate whether DCs secreting IL-18 directly or indirectly modulate differentiation of T cells in NTx–*PD-1*$^{-/-}$ mice, we next examined mRNA expression of IL-18Rα on $CD4^+$ and $CD8^+$ T cells in the spleen and liver. We isolated these cells in the spleen and liver of 2.5-week-old NTx–*PD-1*$^{-/-}$ mice and measured mRNA expression of IL-18Rα. We found that isolated splenic and hepatic $CD4^+$ and $CD8^+$ T cells increased IL-18Rα mRNA expression, suggesting that IL-18 can directly affect differentiation of these cells (Fig. 7D). Interestingly, isolated DCs in the spleen and liver of 2.5-week-old mice expressed upregulated expression of IL-18Rα mRNA (Fig. 7E). In addition, four-week-old NTx–*PD-1*$^{-/-}$ mice injected with anti–IL-18Rβ mAb showed decreased serum levels of IL-18 (Fig. 7F), suggesting that IL-18 may act as an autocrine for differentiation and/or function of proinflammatory IL-18R–expressing DCs. In AIH progression, mRNA expression of IFN-γ and TNF-α in the inflamed liver as well as serum levels of these cytokines were markedly elevated[7-10], so TNF-α could be involved in the maturation of DCs. Indeed, neutralization of TNF-α but not IFN-γ reduced serum levels of IL-18 (Fig. 7F), implying that TNF-α is also directly/indirectly involved in differentiation and/or function of proinflammatory IL-18R–expressing DCs.

Neutralization of IL-18R Signaling Altered Splenic T Cell Function and Ab Production in NTx–PD-1$^{-/-}$ Mice. We found that DCs and T cells, not only in inflamed liver but also in the spleen, expressed IL18Rα in AIH progression (Fig. 7D and 7E). In addition, $CD4^+$ and $CD8^+$ T cells in the spleen predominantly expressed CXCR3 (Fig. 1E).[8] We next examined whether IL-18 is involved in differentiation of splenic T cells in NTx–*PD-1*$^{-/-}$ mice. We found that injecting anti–IL-18Rβ significantly reduced the number of $CXCR3^+$ cells in $CD4^+$ T cells as well as in $CD8^+$ T cells of the spleen in 2.5-week-old NTx–*PD-1*$^{-/-}$ mice (Fig. 8A). In addition, we found that neutralizing IL-18–mediated signaling suppressed expression of T-bet, IFN-γ, TNF-α, and IL-18Rα and upregulated expression of GATA3 in splenic $CD4^+$ T cells (Fig. 8B). Moreover, although production of total immunoglobulin and ANA increased in NTx–*PD-1*$^{-/-}$ mice, injecting anti–IL-18Rβ reduced total immunoglobulin and ANA in the Th1-dependent IgG2a subclass (supplementary Fig.3). In this mouse model, splenic $CD4^+$ T cells showing the T_{FH} cell phenotype were localized in B-cell follicles with huge GCs.[8] Although injections of anti-IL-12p40 did not significantly reduce the size of GCs in the spleen at four weeks, injecting anti-IL-18Rβ mAb induced enlargement of PNA^+ GC in $B220^+$ follicles (supplementary Fig. 4A and 4B). Taken together, these data suggest that DC-derived IL-18 is involved in the differentiation of $CD4^+$T cells into Th1 cells and $CD8^+$ T cells into effector T cells, respectively, in the spleen of NTx–*PD-1*$^{-/-}$ mice.

Discussion

In this study, using our fatal AIH model, we examined molecules key to the triggering of fatal progression of AIH. We found that in the progression, CXCR3 expressing Th1 cells and $CD8^+$ effector T cells infiltrated the liver, $CD8^+$ effector T cells triggering the fatal destruction of the liver; that hepatic macrophages/Kupffer cells producing CXCL9 is critical for migration of these T cells; and that DC-derived IL-18 is critical for differentiation of Th1 cells and $CD8^+$ effector T cells (Fig. 8C).

We previously reported that in the induction phase of AIH in two-week-old NTx–*PD-1*$^{-/-}$ mice, IL-21-producing splenic T_{FH} cells directly migrated into the liver via the CCR6-CCL20 axis, triggering AIH.[8] In contrast, we showed here that in severely inflamed livers in three-week-old NTx–*PD-1*$^{-/-}$ mice, DC-derived IL-18 mediates the differentiation of Th1 cells and $CD8^+$ effector T cells, and CXCR3-CXCL9-axis triggers the migration of these T cells, resulting in fatal AIH progression. Therefore, in the development of fatal AIH in our model, different types of T cells are critically involved at different time points in the induction and fatal progression of AIH. This involvement has also been reported in experimental autoimmune encephalomyelitis (EAE), a $CD4^+$ T cell-mediated disease of the central nervous system.[27] In EAE, Th17 cells migrate via the CCR6-CCL20 axis, triggering inflammation in the induction phase, whereas Th1 cells are mainly involved in inflamed lesions in the central nervous system during active progression.[27] In addition, a recent study reported that T_{FH}-like cells were transiently generated during IL-12-mediating Th1 cell differentiation. In mice infected with *Toxoplasma gondii*, an obligate intracellular parasite, T_{FH}-like cells were generated 7 days after infection, the proportion of T_{FH}-like cells declined, and IFN-γ producing Th1 cells increased at day 15.[19]

In this study, we showed that DC-derived IL-18 is critical for differentiation of Th1 cells and $CD8^+$ effector T cells in AIH progression. IL-18 is known to be produced by various types of immune cells and epithelial cells.[25, 26] In humans, IL-18 produced by DCs promotes Th1 induction.[28] IL-18 stimulates Th1-mediated immune responses and activates Th1 cells, which highly express functional IL-18 receptor, producing large amounts of IFN-γ. [25, 26] In addition, in an atopic dermatitis mouse model, IL-18 could induce differentiation of Th1-like cells that expressed IFN-γ and CXCR3.[29] In humans, IL-18 has been shown to be involved in disease processes associated with excessive Th1 responses in several inflammatory diseases, including autoimmune diseases.[30-32] Patients

with acute hepatitis, chronic liver disease, fulminant hepatitis, primary biliary cirrhosis, or AIH all show elevated serum levels of IL-18[21, 22], which correlates with disease severity.[33, 34]

We found that splenic and hepatic DCs increased IL-18 mRNA expression, together with upregulated expression of NALP3 and, to a lesser extent, IL-1β. However, DCs only secreted IL-18 and induced elevation of serum levels of IL-18. Indeed, administering anti-IL-18Rβ but not anti-IL-1β suppressed fatal AIH. After inflammasome activation via NALP3 occurs in the cells, inactive pro-caspase-1 is activated into active caspase-1. Following cleavage by active caspase-1, mature IL-18 as wells as IL-1β can be secreted from the cells[35]. These canonical IL-1β and IL-18 secretions via inflammasome activation are involved in acetaminophen-induced liver injury[36]. However, several recent studies suggest that secretion of IL-18, but not IL-1β, via the activation of inflammasome and caspase-1 can be orchestrated by several distinct regulatory mechanisms[37-39]. Thus, in NTx–*PD-1*$^{-/-}$ mice, distinct licensing of IL-1β and IL-18 secretion may be involved in the non-canonical secretion of IL-18 via the activation of inflammasome.

Because TNF-α can directly induce the maturation of DCs, TNF-α and IL-18 may directly induce inflammasome upregulation and skew toward IL-18 production via repression of IL-1β transcript but upregulation of IL-18 transcript. On the other hand, TNF-α directly and indirectly induces cell death of hepatocytes[40] and free DNA released from apoptotic hepatocytes can activate Tlr9, triggering a signaling cascade to induce pro-IL-1β and pro-IL-18[36]. Therefore, TNF-α may induce apoptosis of hepatocytes, triggering canonical IL-18 production initially. However, IL-18 may act as an autocrine for skewing prolonged IL-18 secretion in DCs.

Although first described as IFN-γ-inducing factor, IL-18 may not make a major contribution to elevated serum levels of IFN-γ in AIH progression. In contrast to IL-18, serum levels of IFN-γ reached the maximal level at one week of age before AIH development; the elevated serum level of IFN-γ gradually decreased during AIH progression.[9] Indeed, IFN-γ was dispensable for upregulating CXCL9 in the liver. Neutralizing IFN-γ did not prevent the development of AIH and induced increased T-cell proliferation in the spleen and liver, resulting in exacerbated T-cell infiltration in AIH[9]. So although IFN-γ generally acts as a critical proinflammatory mediator, it exerts regulatory functions to limit tissue damage associated with inflammation of AIH in

progression.

We showed here that the migration of exclusively CXCR3-expressing T cells was triggered by hepatic macrophages/Kupffer cells producing one CXCR3 ligand, CXCL9. Although CXCL9, CXCL10, and CXCL11 can bind to the common receptor CXCR3, differences have been reported in the kinetics and the tissue/cell type expression patterns of these three chemokine genes and their proteins during infection or inflammatory responses.[41-44] Studies using CXCL9- or CXCL10-deficient mice have shown the non-redundant function of these chemokines in various immunoinflammatory settings, including a hepatitis B virus (HBV) transgenic mouse model and a liver injury model.[41-44]

In this study, we showed that CXCL9-expressing cells are macrophages/Kupffer cells in AIH progression. Although rIFN-γ and rTNF-α upregulated hepatic CXCL9 expression, anti–IFN-γ did not suppress hepatic CXCL9 upregulation. In NTx–*PD-1*$^{-/-}$ mice, cell types responsible for secreting CXCR3 ligands in various organs may exhibit a refractory response to constitutively elevated serum IFN-γ. In addition, TNF-α secreted in autocrine and in paracrine fashion by activated T cells may induce uncontrollable CXCL9 expression in AIH progression. Therefore, anti–TNF-α monotherapy may not significantly prevent fatal AIH in mice.

In conclusion, we have identified the pivotal role of the IL-18 and CXCR3-CXCL9 axis in fatal progression of AIH, implying that blocking these systems may have clinical potential for protecting against fatal progression of this disease.

References

1. Nikias GA, Batts KP, Czaja AJ. The nature and prognostic implications of autoimmune hepatitis with an acute presentation. J Hepatol 1994 ;21:866-71.
2. Yamamoto K, Miyake Y, Ohira H, Suzuki Y, Zeniya M, Onji M, et al. Prognosis of autoimmune hepatitis showing acute presentation. Hepatol Res. 2013;43(6):630-8.
3. Soloway RD, Summerskill WH, Baggenstoss AH, Geall MG, Gitnićk GL, Elveback IR, et al. Clinical, biochemical, and histological remission of severe chronic active liver disease: a controlled study of treatments and early prognosis. Gastroenterology 1972;63:820-33.
4. Verma S, Torbenson M, Thuluvath PJ. The impact of ethnicity on the natural history of autoimmune hepatitis. Hepatology 2007;46:1828-35.
5. Verma S, Maheshwari A, Thuluvath P. Liver failure as initial presentation of autoimmune hepatitis: clinical characteristics, predictors of response to steroid therapy, and outcomes. Hepatology 2009;49:1396-7.
6. Manns MP, Czaja AJ, Gorham JD, Krawitt EL, Mieli-Vergani G, Vergani D, et al. Diagnosis and management of autoimmune hepatitis. Hepatology 2010;51:2193-213.
7. Kido M, Watanabe N, Okazaki T, Akamatsu T, Tanaka J, Saga K, et al. Fatal autoimmune hepatitis induced by concurrent loss of naturally arising regulatory T cells and PD-1-mediated signaling. Gastroenterology 2008:135:1333-43.
8. Aoki N, Kido M, Iwamoto S, Nishiura H, Maruoka R, Tanaka J, et al. Dysregulated generation of follicular helper T cells in the spleen triggers fatal autoimmune hepatitis in mice. Gastroenterology 2011;140:1322-33.
9. Iwamoto S, Kido M, Aoki N, Nishiura H, Maruoka R, Ikeda A, et al. IFN-γ is reciprocally involved in the concurrent development of organ-specific autoimmunity in the liver and stomach. Autoimmunity 2012;45:186-98.
10. Iwamoto S, Kido M, Aoki N, Nishiura H, Maruoka R, Ikeda A, et al. TNF-α is essential in the induction of fatal autoimmune hepatitis in mice through upregulation of hepatic CCL20 expression. Clin Immunol. 2013;146(1):15-25.
11. Maruoka R, Aoki N, Kido M, Iwamoto S, Nishiura H, Ikeda A, et al. Splenectomy prolongs the effects of corticosteroids in mouse models of autoimmune hepatitis. Gastroenterology. 2013;145:209-220.

12. King C. New insights into the differentiation and function of T follicular helper cells. Nat Rev Immunol 2009;9:757-66.
13. Nishimura H, Okazaki T, Tanaka Y, Nakatani K, Hara M, Matsumori A, et al. Autoimmune dilated cardiomyopathy in PD-1 receptor-deficient mice. Science 2001;291:319-22.
14. Liu L, Callahan MK, Huang D, Ransohoff RM. Chemokine receptor CXCR3: an unexpected enigma. Curr Top Dev Biol 2005;68:149-81.
15. Groom JR, Luster AD. CXCR3 in T cell function. Exp Cell Res 2011;317: 620-31.
16. Lacotte S, Brun S, Muller S, Dumortier H. CXCR3, inflammation, and autoimmune diseases. Ann N Y Acad Sci 2009;1173: 310-7.
17. Lee EY, Lee ZH, Song YW. CXCL10 and autoimmune diseases. Autoimmun Rev 2009;8:379-83.
18. Szabo SJ, Sullivan BM, Peng SL, Glimcher LH. Molecular mechanisms regulating Th1 immune responses. Annu Rev Immunol 2003;21:713-58.
19. Nakayamada S, Kanno Y, Takahashi H, Jankovic D, Lu KT, Johnson TA, et al. Early Th1 cell differentiation is marked by a Tfh cell-like transition. Immunity 2011;35:919-31.
20. Wenner CA, Güler ML, Macatonia SE, O'Garra A, Murphy KM. Roles of IFN-γ and IFN-γ in IL-12-induced T helper cell-1 development. J Immunol 1996;156:1442–7.
21. Yamano T, Higashi T, Nouso K, Nakatsukasa H, Kariyama K, Yumoto E, et al. Serum interferon-gamma-inducing factor/IL-18 levels in primary biliary cirrhosis. Clin Exp Immunol 2000;122:227-31.
22. Yumoto E, Higashi T, Nouso K, Nakatsukasa H, Fujiwara K, Hanafusa T, et al. Serum gamma-interferon-inducing factor (IL-18) and IL-10 levels in patients with acute hepatitis and fulminant hepatic failure. J Gastroenterol Hepatol 2002;17:285-94.
23. Tsutsui H, Kayagaki N, Kuida K, Nakano H, Hayashi N, Takeda K, et al. Caspase-1-independent, Fas/Fas ligand-mediated IL-18 secretion from macrophages causes acute liver injury in mice. Immunity 1999;11:359-67.
24. Faggioni R, Jones-Carson J, Reed DA, Dinarello CA, Feingold KR, Grunfeld C, et al. Leptin-deficient (ob/ob) mice are protected from T cell-mediated hepatotoxicity: role of tumor necrosis factor α and IL-18. Proc Natl Acad Sci

USA 2000;97:2367-72.

25. Reddy P. Interleukin-18: recent advances. Curr Opin Hematol 2004;11:405-10.
26. Arend WP, Palmer G, Gabay C. IL-1, IL-18, and IL-33 families of cytokines. Immunol Rev 2008;223:20-38.
27. Reboldi A, Coisne C, Baumjohann D, Benvenuto F, Bottinelli D, Lira S, et al. C-C chemokine receptor 6-regulated entry of TH-17 cells into the CNS through the choroid plexus is required for the initiation of EAE. Nat Immunol 2009;10:514-23.
28. Kaser A, Kaser S, Kaneider NC, Enrich B, Wiedermann CJ, Tilg H. Interleukin-18 attracts plasmacytoid dendritic cells (DC2s) and promotes Th1 induction by DC2s through IL-18 receptor expression. Blood 2004;103(2):648-55.
29. Terada M, Tsutsui H, Imai Y, Yasuda K, Mizutani H, Yamanishi K, et al. Contribution of IL-18 to atopic-dermatitis-like skin inflammation induced by Staphylococcus aureus product in mice. Proc Natl Acad Sci USA 2006;103:8816-21.
30. Calvani N, Tucci M, Richards HB, Tartaglia P, Silvestris F. Th1 cytokines in the pathogenesis of lupus nephritis: the role of IL-18. Autoimmun Rev 2005;4:542-8.
31. Dinarello CA. Interleukin-18 and the pathogenesis of inflammatory diseases. Semin Nephrol 2007;27:98-114.
32. Wittmann M, Macdonald A, Renne J. IL-18 and skin inflammation. Autoimmun Rev 2009;9:45-8.
33. Sharma A, Chakraborti A, Das A, Dhiman RK, Chawla Y. Elevation of interleukin-18 in chronic hepatitis C: implications for hepatitis C virus pathogenesis. Immunology 2009;128:e514-22.
34. Ludwiczek O, Kaser A, Novick D, Dinarello CA, Rubinstein M, Vogel W, et al. Plasma levels of interleukin-18 and interleukin-18 binding protein are elevated in patients with chronic liver disease. J Clin Immunology 2002;22(6):331-7.
35. Franchi L, Eigenbrod T, Muñoz-Planillo R, Nuñez G. The inflammasome: a caspase-1-activation platform that regulates immune responses and disease pathogenesis. Nat Immunol. 2009;10(3):241-7.
36. Imaeda AB, Watanabe A, Sohail MA, Mahmood S, Mohamadnejad M, Sutterwala FS, et al. Acetaminophen-induced hepatotoxicity in mice is dependent on Tlr9 and the Nalp3 inflammasome. J Clin Invest. 2009;119(2):305-14.
37. Kahlenberg JM, Thacker SG, Berthier CC, Cohen CD, Kretzler M, Kaplan MJ.

Inflammasome activation of IL-18 results in endothelial progenitor cell dysfunction in systemic lupus erythematosus. J Immunol. 2011 Dec 1;187(11):6143-56.

38. Schmidt RL, Lenz LL. Distinct licensing of IL-18 and IL-1β secretion in response to NLRP3 inflammasome activation. PLoS One. 2012;7(9):e45186.
39. Jitprasertwong P, Jaedicke KM, Nile CJ, Preshaw PM, Taylor JJ. Leptin enhances the secretion of interleukin (IL)-18, but not IL-1β, from human monocytes via activation of caspase-1. Cytokine. 2014;65(2):222-230.
40. Schwabe RF, Brenner DA. Mechanisms of Liver Injury. I. TNF-alpha-induced liver injury: role of IKK, JNK, and ROS pathways. Am J Physiol Gastrointest Liver Physiol. 2006;290(4):G583-9.
41. Mach F, Sauty A, Iarossi AS, Sukhova GK, Neote K, Libby P, et al. Differential expression of three T lymphocyte-activating CXC chemokines by human atheroma-associated cells. J Clin Invest 1999;104:1041-50.
42. Kakimi K, Lane TE, Wieland S, Asensio VC, Campbell IL, Chisari FV, et al. Blocking chemokine responsive to γ-2/interferon (IFN)- γ inducible protein and monokine induced by IFN- γ activity in vivo reduces the pathogenetic but not the antiviral potential of hepatitis B virus-specific cytotoxic T lymphocytes. J Exp Med 2001;194:1755-66.
43. Zhai Y, Shen XD, Gao F, Zhao A, Freitas MC, Lassman C, et al. CXCL10 regulates liver innate immune response against ischemia and reperfusion injury. Hepatology 2008;47: 207-14.
44. Menke J, Zeller GC, Kikawada E, Means TK, Huang XR, Lan HY, et al. CXCL9, but not CXCL10, promotes CXCR3-dependent immune-mediated kidney disease. J Am Soc Nephrol 2008;19:1177-89.

Figure Legends

Fig. 1. Histological and immunological analysis of AIH-bearing NTx–*PD-1*$^{-/-}$ mice. (A) Histological findings of the liver in NTx–*PD-1*$^{-/-}$ mice at indicated ages in weeks. All scale bars, 100 μm. (B and C) Livers from 3-week-old *PD-1*$^{-/-}$ mice with or without NTx were used for real-time quantitative RT-PCR analyses for mRNA expressions of lineage-specific transcription factors such as T-bet, GATA-3, or ROR-γt, and various cytokines (B) and Th1-cell–expressing chemokine receptor CXCR3 (C). (D) Cell numbers of $CD4^+$ and $CD8^+$ T cells in the spleen, liver, and mesenteric lymph nodes (MLN) of *PD-1*$^{-/-}$ mice with or without NTx at the indicated age. Isolated cells were stained with FITC-anti-CD3e and APC-Cy7-anti-CD4 or APC-anti-CD8. (E) Cell numbers of splenic and hepatic $CD8^+$ T cells expressing indicated chemokine receptors. Isolated cells were stained with FITC-anti-CD3e, APC-anti-CD8 and PE-anti-CCR6, -anti-CCR9, or -anti-CXCR3. Flow cytometric analyses were carried out as described in Supplementary Materials and Methods. Numbers of indicated T cell populations were calculated by (percentage of the cells in viable cells) x (no. of viable cells). Data are shown as the mean of at least three mice. *Error bars* represent SD. *Asterisks* indicate $P < 0.05$. n.s., not significant. ND, not detected.

Fig. 2. Immunological and histological analysis for NTx–*PD-1*$^{-/-}$ mice injected with anti-CD8 in the progression phase of AIH. (A) NTx–*PD-1*$^{-/-}$ mice at 14 days after thymectomy were injected intraperitoneally (i.p.) every week with 100 μg of depletion antibody to CD8 (n=6) or the isotype control mAb (n=6). After two injections, mice at four weeks of age were sacrificed. (B) Cell numbers of $CD8^+$ T cells in the spleen of NTx–*PD-1*$^{-/-}$ mice injected with indicated Abs. (C) Survival rates at four weeks of age. (D) Representative stainings of the liver for hematoxylin and eosin are shown. (E) Cell numbers of infiltrating T cells in the liver of NTx–*PD-1*$^{-/-}$ mice injected with indicated Abs. Isolated cells were stained with FITC-anti-CD3e and APC-Cy7-anti-CD4 or APC-anti-CD8. *Error bars* represent SD. *Asterisks* indicate $P < 0.05$.

Fig. 3. Expression levels of CXCR3 ligands in NTx–*PD-1*$^{-/-}$ mice. (A) Livers from 3-week-old *PD-1*$^{-/-}$ and *PD-1*$^{+/+}$ mice with or without NTx were used for real-time quantitative RT-PCR analyses for mRNA expressions of CXCR3 ligands, CXCL9, CXCL10, and CXCL11. (B) CXCL9 mRNA expression in various organs. The stomach,

heart, lung, intestine, pancreas and kidney were from 3-week-old *PD-1*$^{-/-}$ mice with or without NTx. (C) Immunostaining with anti-CXCL9, CXCL10, or isotype controls. The livers from three-week-old *PD-1*$^{-/-}$ and *PD-1*$^{+/+}$ mice with or without NTx were used. (D) Serum levels of CXCL9 and CXCL10 were measured by ELISA. Data are shown of sera from indicated aged *PD-1*$^{-/-}$ and *PD-1*$^{+/+}$ mice with or without NTx. Data are shown as the mean of at least three mice. *Error bars* represent SD. *Asterisks* indicate $P < 0.05$. n.s., not significant. Scale bars, 100 μm.

Fig. 4. Survival rate and histological analysis of the liver in NTx–*PD-1*$^{-/-}$ mice injected with neutralizing Abs for CXCR3 ligands. (A and B) NTx–*PD-1*$^{-/-}$ mice at one day after thymectomy were injected intraperitoneally every week with 100 μg of neutralizing anti-CXCL9 (n=5), anti-CXCL10 (n=5) or the isotype control mAbs (n=5). Survival rates at four weeks of age. (C) After four injections of anti-CXCL9, anti-CXCL10 or a combination with anti-CXCL9 and anti-CXCL10 (n=5), mice at four weeks of age were sacrificed, and the livers were harvested. Representative stainings of the liver for hematoxylin and eosin (HE), CD4, and CD8 are shown. Upper panels are control stainings of the liver in *PD-1*$^{-/-}$ mice with or without NTx. *Asterisks* indicate $P < 0.05$. n.s., not significant. All *scale bars*, 100 μm.

Fig. 5. The cellular source of CXCL9 and the role of cytokines in inducting CXCR3 ligands in NTx–PD-1$^{-/-}$ mice. (A) Immunostaining with anti-CXCL9, F4/80, CD4, and CD8. The livers from 3-week-old NTx–*PD-1*$^{-/-}$ mice were used. Scale bars, 20μm. (B) Four-week-old *PD-1*$^{-/-}$ mice were injected intraperitoneally (i.p.) with 10 μg/kg of mouse rIFNγ or rTNFα. The livers at the indicated time after injection were subjected to real-time quantitative RT-PCR analyses for mRNA expressions of CXCL9 and CXCL10. (C) NTx–*PD-1*$^{-/-}$ mice at one day after thymectomy were injected intraperitoneally every week with 100 μg of neutralizing anti-IFNγ, anti-TNFα, or isotype controls. After four injections, mice at four weeks of age were sacrificed. *PD-1*$^{-/-}$ mice without NTx at the same age were used for controls. The livers from these mice were used for real-time quantitative RT-PCR analyses for mRNA expressions of CXCL9. (D, E) NTx–*PD-1*$^{-/-}$ mice at fourteen day after thymectomy were injected intraperitoneally every week with 100 μg of neutralizing anti-TNFα or isotype control. After two injections, mice at four weeks of age were sacrificed. Liver stainings are shown for hematoxylin and eosin, and

immunostaining with anti-TNFα. Scale bars, 50 μm (upper four panels). Immunostaining with anti-TNFα and anti-CXCL9. Scale bars, 20 μm (lower four panels) (D). Serum levels of CXCL9 were measured by ELISA (E). Data are shown as the mean of at least three mice. *Error bars* represent SD. *Asterisks* indicate $P < 0.05$. n.s., not significant.

Fig. 6. Serum levels of IL-18 and IL1-β, and analysis for NTx–*PD-1*$^{-/-}$ mice injected with blocking Abs for IL-18R signaling and neutralizing Abs for IL-1β. (A, B) Serum levels of IL-18 at indicated ages and IL-1β at 3 weeks of age of *PD-1*$^{-/-}$ mice with or without NTx were measured by ELISA. (C, E, F) NTx–*PD-1*$^{-/-}$ mice at one day after thymectomy were injected intraperitoneally every week with 100 μg of IL-18Rβ mAb (n=10), or the isotype control mAb (n=10). (D) NTx–*PD-1*$^{-/-}$ mice were injected with 100 μg of IL-1β mAb (n=3), or the isotype control mAb (n=3) as described above. After four injections, mice at four weeks of age were sacrificed. Stainings of the liver for hematoxylin and eosin (HE), CD4, and CD8 (C, D), serum levels of AST and ALT (E) and survival rates at four weeks of age (F) are shown. Data are shown as the mean of at least three mice. *Error bars* represent SD. *Asterisks* indicate $P < 0.05$. n.s., not significant. Scale bars, 100 μm.

Fig. 7. Expression levels of IL-18, IL-1β, NALP3, and IL-18Rα in AIH-bearing 2.5-week-old NTx–*PD-1*$^{-/-}$ mice. (A) Expression levels of mRNA encoding IL-18 of $CD3^+CD4^+$ T cells, $CD3^+CD8^+$ T cells, $B220^+$ B cells, $CD11b^+CD11c^-$ macrophages, $CD11c^+$ DCs and $CD3^-DX5^+$ NK cells in the spleen and liver of 2.5-week-old NTx–*PD-1*$^{-/-}$ mice. Data represent 1 of 3 independent experiments. (B) Expression levels of mRNA encoding IL-1β and NALP3 of $CD11c^+$ DCs in the spleen of 2.5-week-old NTx–PD-1$^{-/-}$ mice. (C) Concentration of IL-18 in DC-culture supernatants measured by ELISA. $CD11c^+$ DCs were isolated from the spleen in *PD-1*$^{-/-}$ mice with or without NTx and DCs were cultured for 24 h. Data are shown as the mean of triplicates. (D and E) Expression levels of mRNA encoding IL-18Rα of $CD3^+CD4^+$ and $CD3^+CD8^+$ T cells (D), and $CD11c^+$ DCs (E) in the spleen and liver of 2.5-week-old NTx–*PD-1*$^{-/-}$ mice. (F) Serum levels of IL-18 were measured by ELISA. NTx–*PD-1*$^{-/-}$ mice at one day after thymectomy were injected intraperitoneally every week with 100 μg of neutralizing anti-IL-18Rβ, anti-IFN, or anti-TNFα. After four injections, mice at four weeks of age

were sacrificed. Data is shown of sera from *PD-1*$^{-/-}$ mice of 4-week-old with indicated condition. Data are shown as the mean of at least three mice. *Error bars* represent SD. *Asterisks* indicate $P < 0.05$. n.s., not significant. ND, not detected.

Fig. 8. Immunological and RT-PCR analysis for NTx–*PD-1*$^{-/-}$ mice injected with blocking Abs for IL-18R signaling, and the model of pathological mechanisms in the progression phase of AIH in NTx–*PD-1*$^{-/-}$ mice. (A-B) NTx–*PD-1*$^{-/-}$ mice at one day after thymectomy were injected with IL-18Rβ mAb. (A) After four injections, mice at four weeks of age were sacrificed as described in Fig 6. Cell numbers of $CXCR3^+$ cells in $CD4^+$ and $CD8^+$ T cells in the spleen. Data are shown as the mean of at least three mice. (B) After three injections, mice at three weeks of age were sacrificed, and $CD4^+$ T cells were isolated from the spleens. Expression levels of mRNA encoding T-bet, GATA-3, ROR-γt, IFNγ, TNFα, and IL-18Rα were measured. Data are shown as the mean of triplicates. *Error bars* represent SD. *Asterisks* indicate $P < 0.05$. n.s., not significant. (C) The model of mechanistic links of cytokines and chemokines in the progression phase of NTx–*PD-1*$^{-/-}$ mice. In the progression, DC-derived IL-18 is critical for differentiation of CXCR3-expressing Th1 cells (Th1) and $CD8^+$ effector T cells (T_E). CXCL9 production by hepatic macrophages/Kupffer cells triggers migration of these T cells into the liver. CXCR3-expressing T_E and, to a lesser extent, Th1 infiltrate the liver and T_E trigger the fatal destruction of the liver.

Fig. 1.

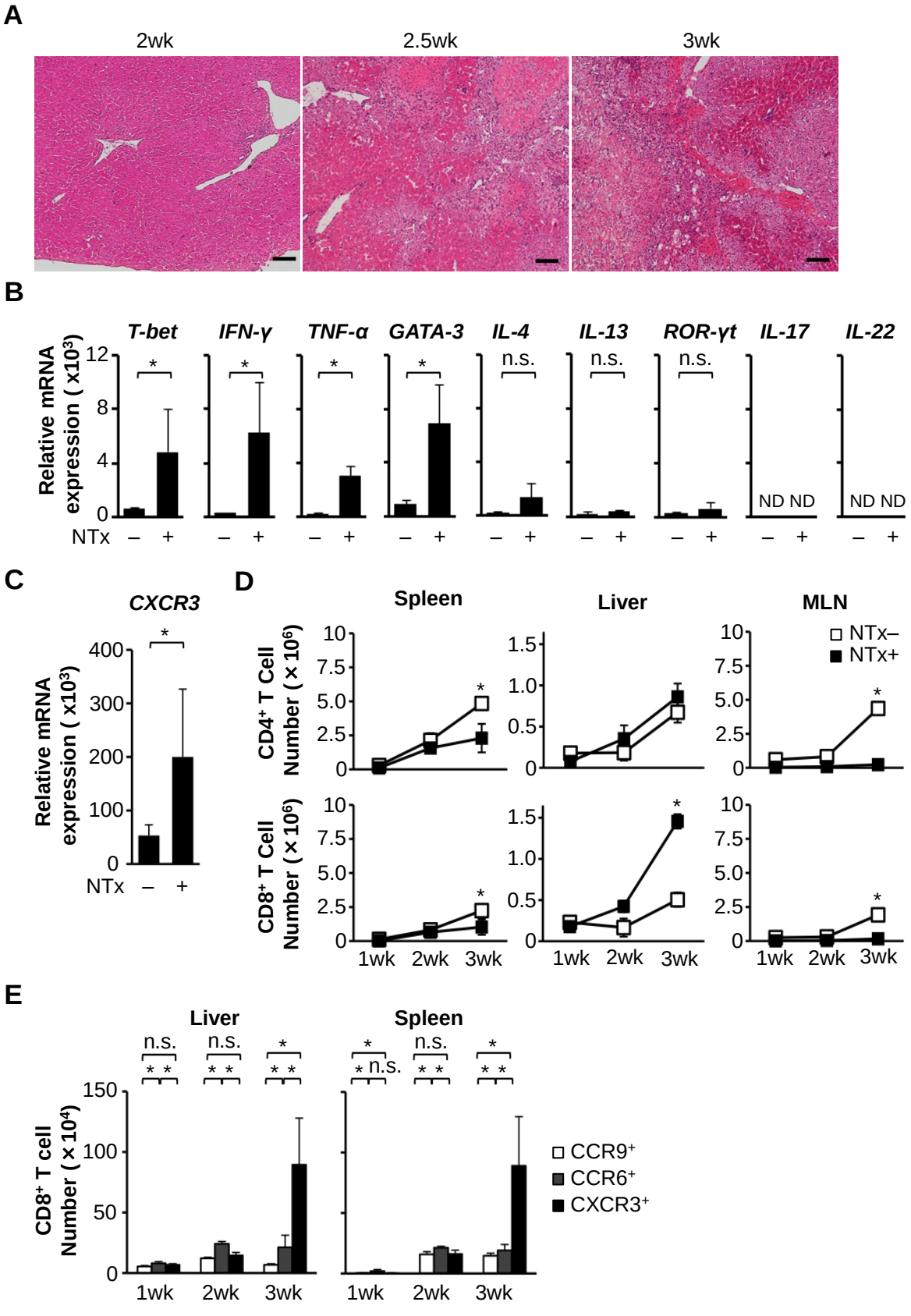
A
2wk
2.5wk
3wk
B
T-bet
IFN-γ
TNF-α
GATA-3
IL-4
IL-13
RORγt
IL-17
IL-22
Relative mRNA expression (x10³)
n.s.
ND ND
NTx – + – + – + – + – + – + – + – + – +
C
CXCR3
Relative mRNA expression (x10³)
NTx – +
D
Spleen
Liver
MLN
CD4⁺ T Cell Number (x 10⁶)
CD8⁺ T Cell Number (x 10⁶)
NTx–
NTx+
1wk 2wk 3wk
E
Liver
Spleen
n.s.
CD8⁺ T cell Number (x 10⁴)
CCR9⁺
CCR6⁺
CXCR3⁺
1wk 2wk 3wk

Fig. 2.

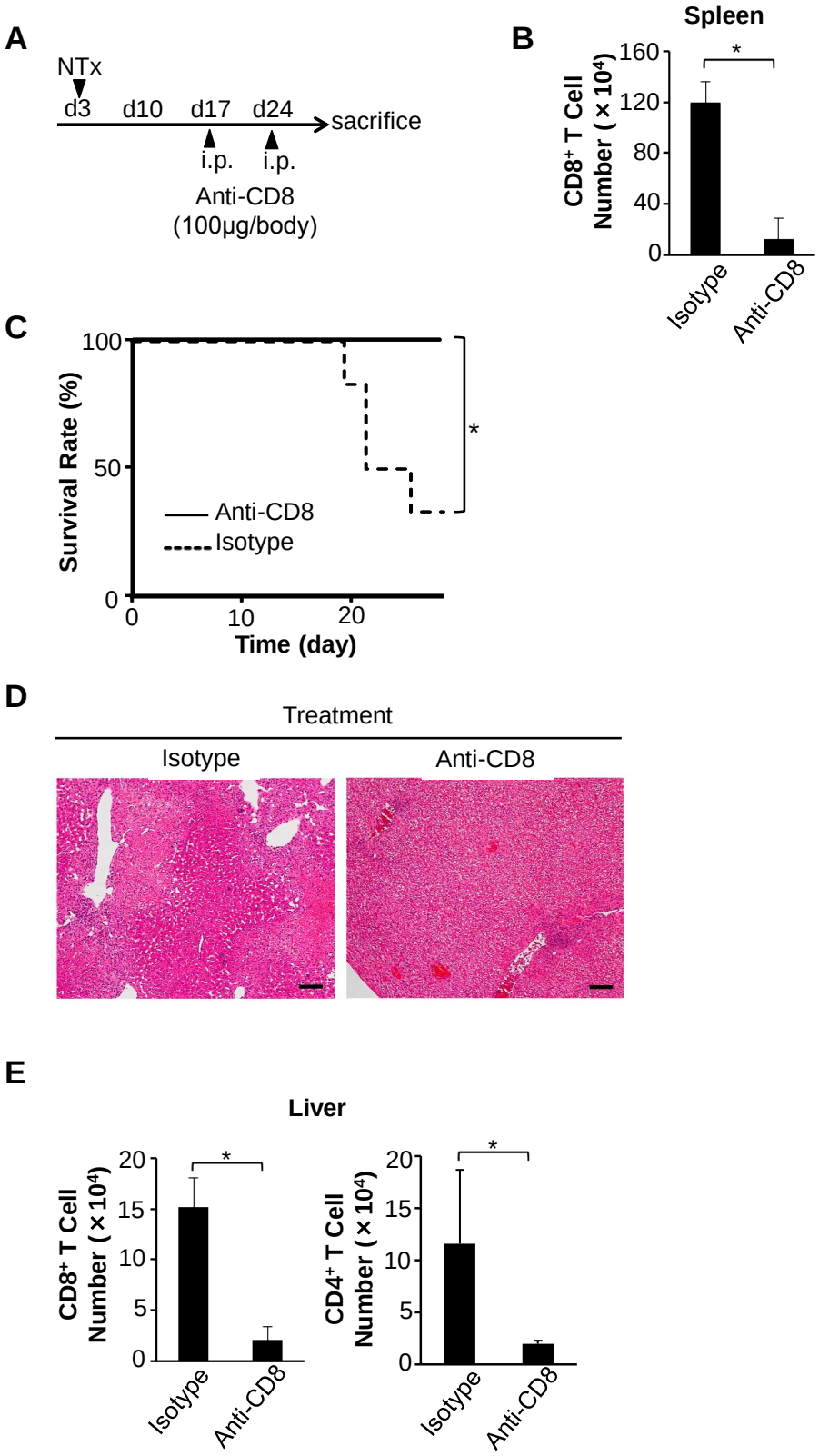
A
NTx
d3
d10
d17
d24
sacrifice
i.p.
i.p.
Anti-CD8
(100μg/body)
B
Spleen
CD8+ T Cell Number (×10⁴)
160
120
80
40
0
*
Isotype
Anti-CD8
C
Survival Rate (%)
100
50
0
0
10
20
Time (day)
Anti-CD8
Isotype
*
D
Treatment
Isotype
Anti-CD8
E
Liver
CD8+ T Cell Number (×10⁴)
20
15
10
5
0
*
Isotype
Anti-CD8
CD4+ T Cell Number (×10⁴)
20
15
10
5
0
*
Isotype
Anti-CD8

Fig. 3.

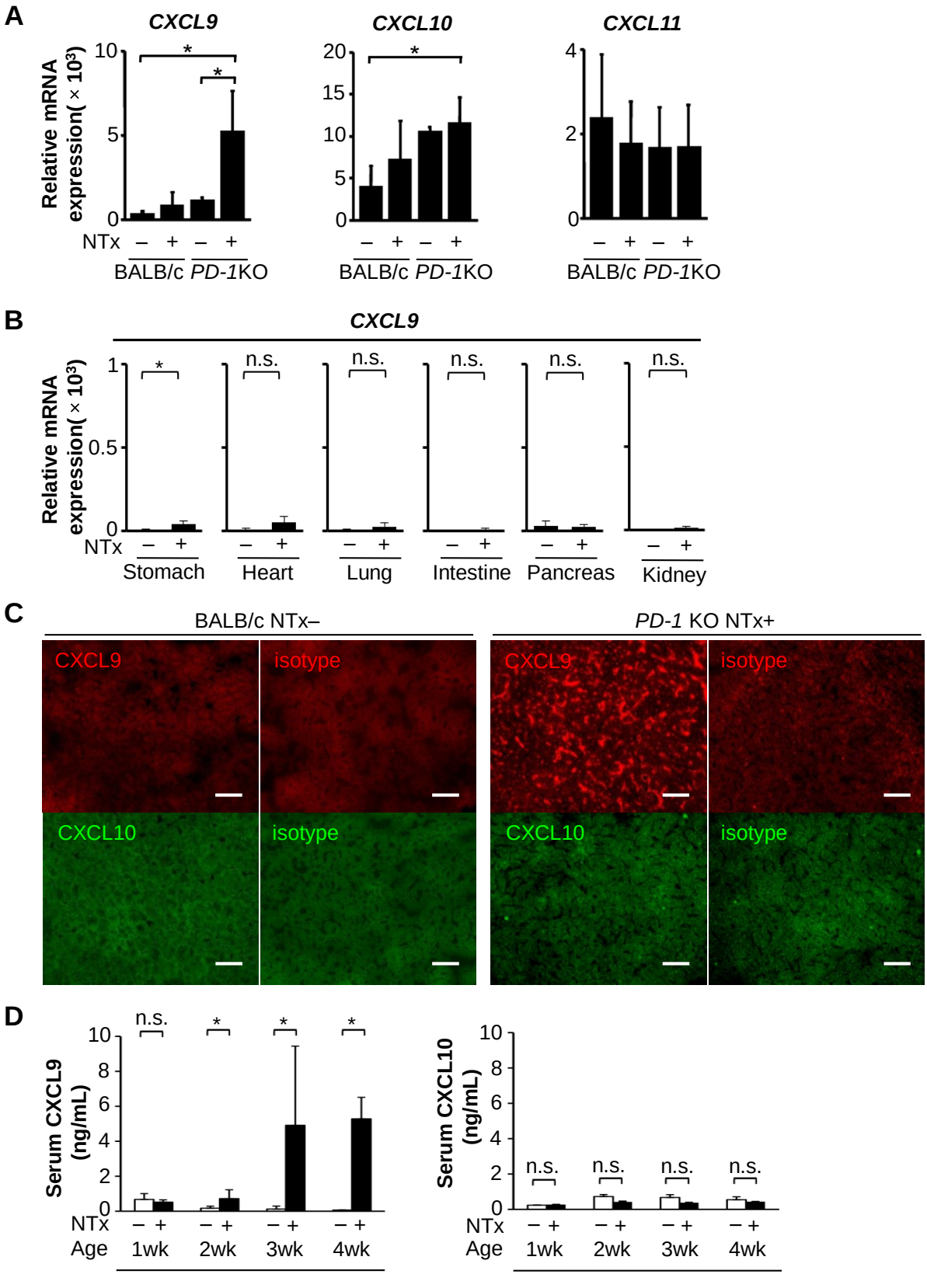
A
CXCL9
CXCL10
CXCL11
Relative mRNA expression(× 10³)
NTx
BALB/c
PD-1KO
B
CXCL9
n.s.
Stomach
Heart
Lung
Intestine
Pancreas
Kidney
C
BALB/c NTx–
PD-1 KO NTx+
CXCL9
isotype
CXCL10
D
Serum CXCL9 (ng/mL)
Serum CXCL10 (ng/mL)
Age
1wk
2wk
3wk
4wk

Fig. 4.

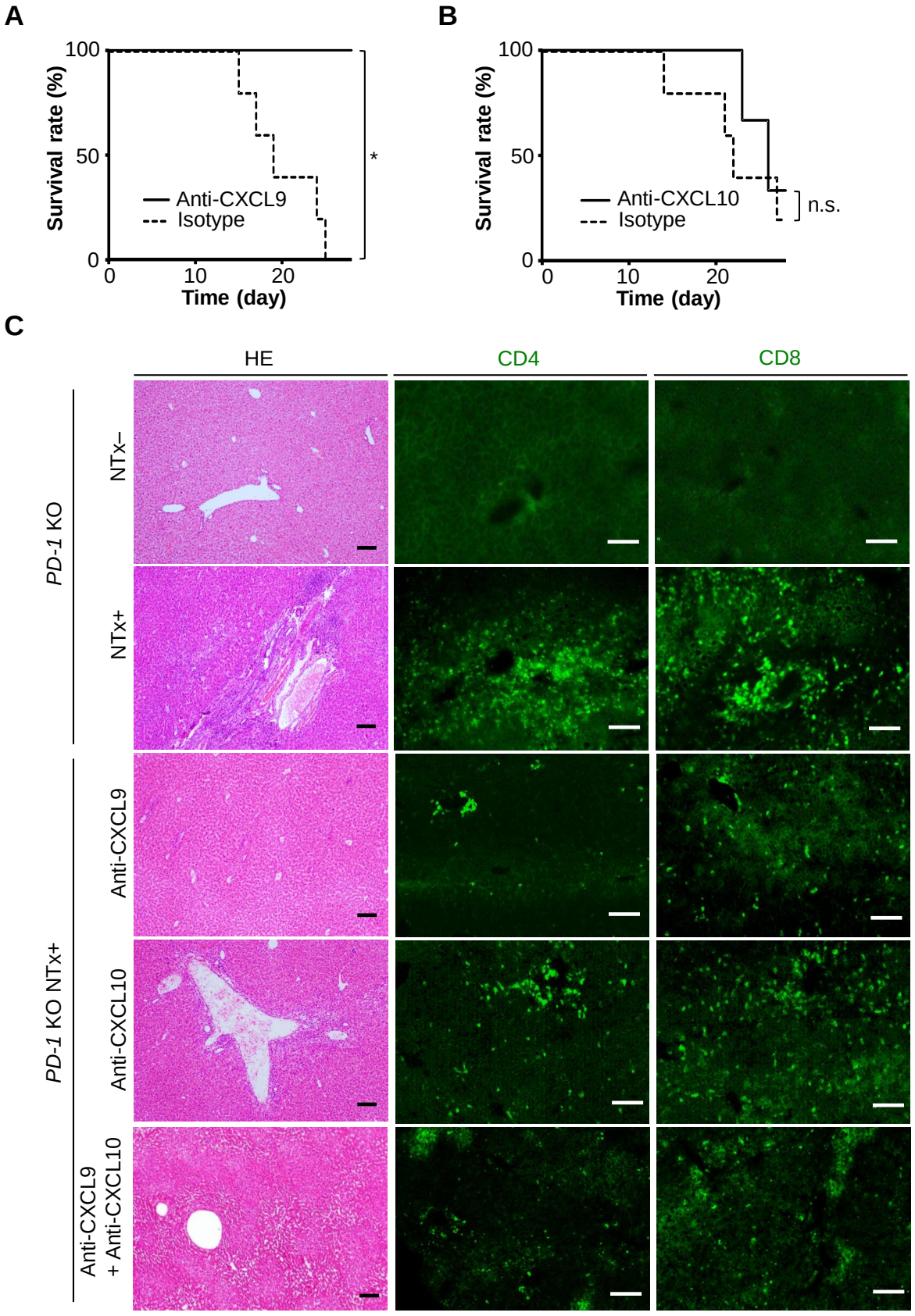
A
100
50
0
Survival rate (%)
Anti-CXCL9
Isotype
*
0
10
20
Time (day)
B
100
50
0
Survival rate (%)
Anti-CXCL10
Isotype
n.s.
0
10
20
Time (day)
C
HE
CD4
CD8
PD-1 KO
NTx–
NTx+
PD-1 KO NTx+
Anti-CXCL9
Anti-CXCL10
Anti-CXCL9
+ Anti-CXCL10

Fig. 5.

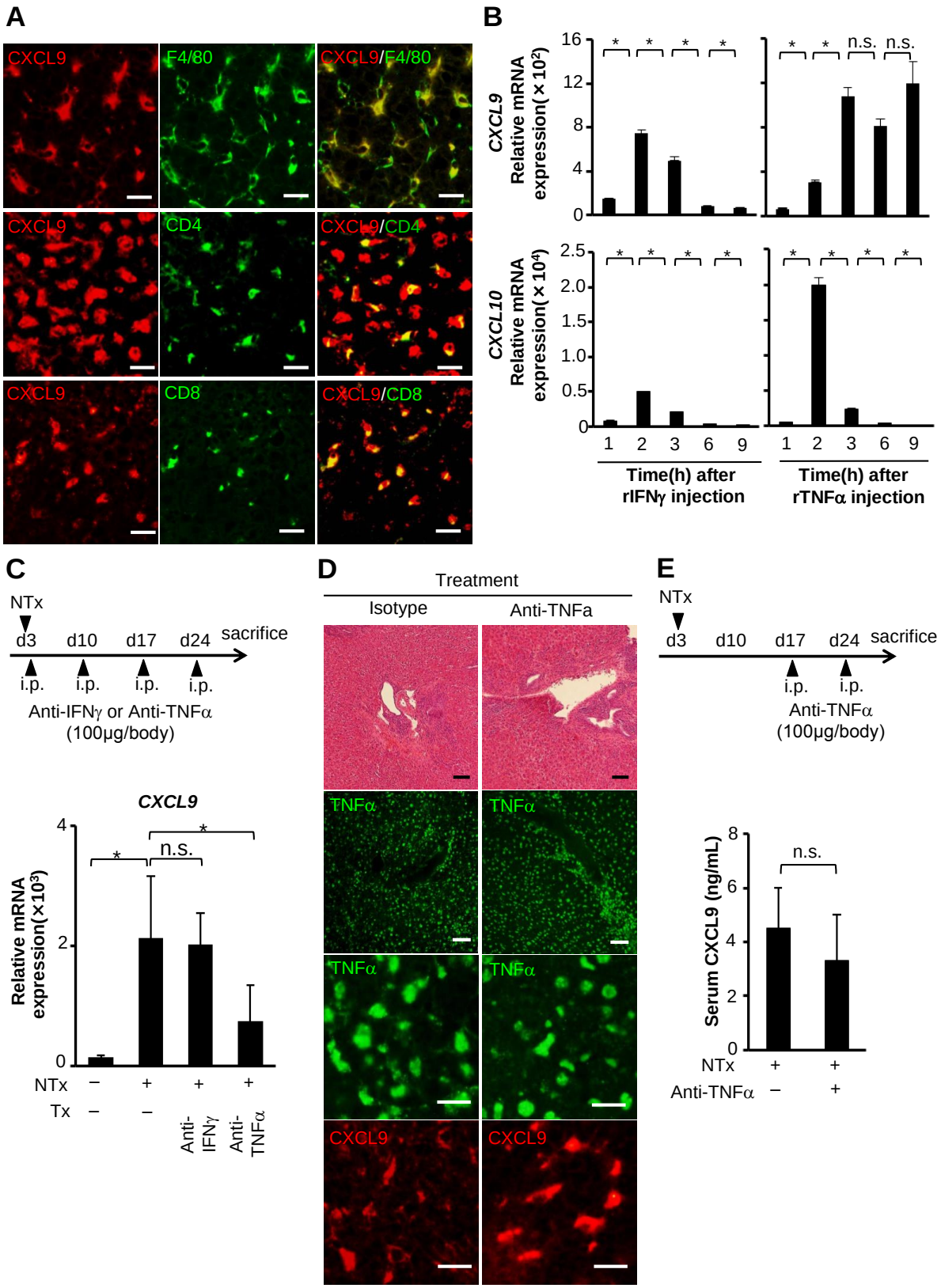
A
CXCL9
F4/80
CXCL9/F4/80
CXCL9
CD4
CXCL9/CD4
CXCL9
CD8
CXCL9/CD8
B
CXCL9 Relative mRNA expression(×10²)
CXCL10 Relative mRNA expression(×10⁴)
n.s.
Time(h) after rIFNγ injection
Time(h) after rTNFα injection
C
NTx
d3
d10
d17
d24
sacrifice
i.p.
Anti-IFNγ or Anti-TNFα (100μg/body)
CXCL9
Relative mRNA expression(×10³)
NTx
Tx
Anti-IFNγ
Anti-TNFα
D
Treatment
Isotype
Anti-TNFa
TNFα
CXCL9
E
NTx
d3
d10
d17
d24
sacrifice
i.p.
Anti-TNFα (100μg/body)
Serum CXCL9 (ng/mL)
n.s.
NTx
Anti-TNFα

Fig. 6.

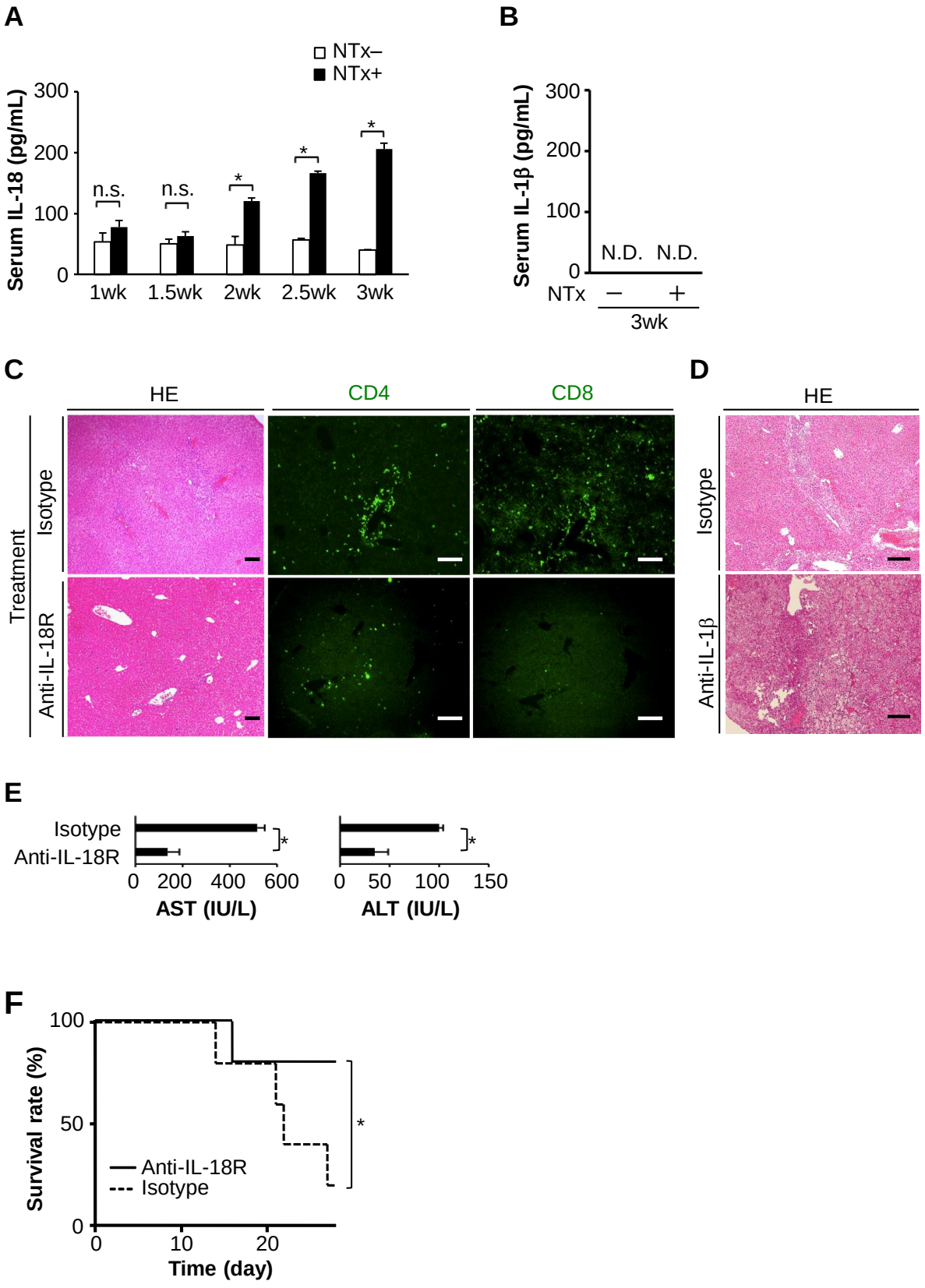
A
NTx–
NTx+
Serum IL-18 (pg/mL)
300
200
100
0
n.s.
n.s.
*
*
*
1wk
1.5wk
2wk
2.5wk
3wk
B
Serum IL-1β (pg/mL)
300
200
100
0
N.D.
N.D.
NTx
–
+
3wk
C
HE
CD4
CD8
Treatment
Isotype
Anti-IL-18R
D
HE
Isotype
Anti-IL-1β
E
Isotype
Anti-IL-18R
*
*
0
200
400
600
AST (IU/L)
0
50
100
150
ALT (IU/L)
F
Survival rate (%)
100
50
0
Anti-IL-18R
Isotype
*
0
10
20
Time (day)

Fig. 7.

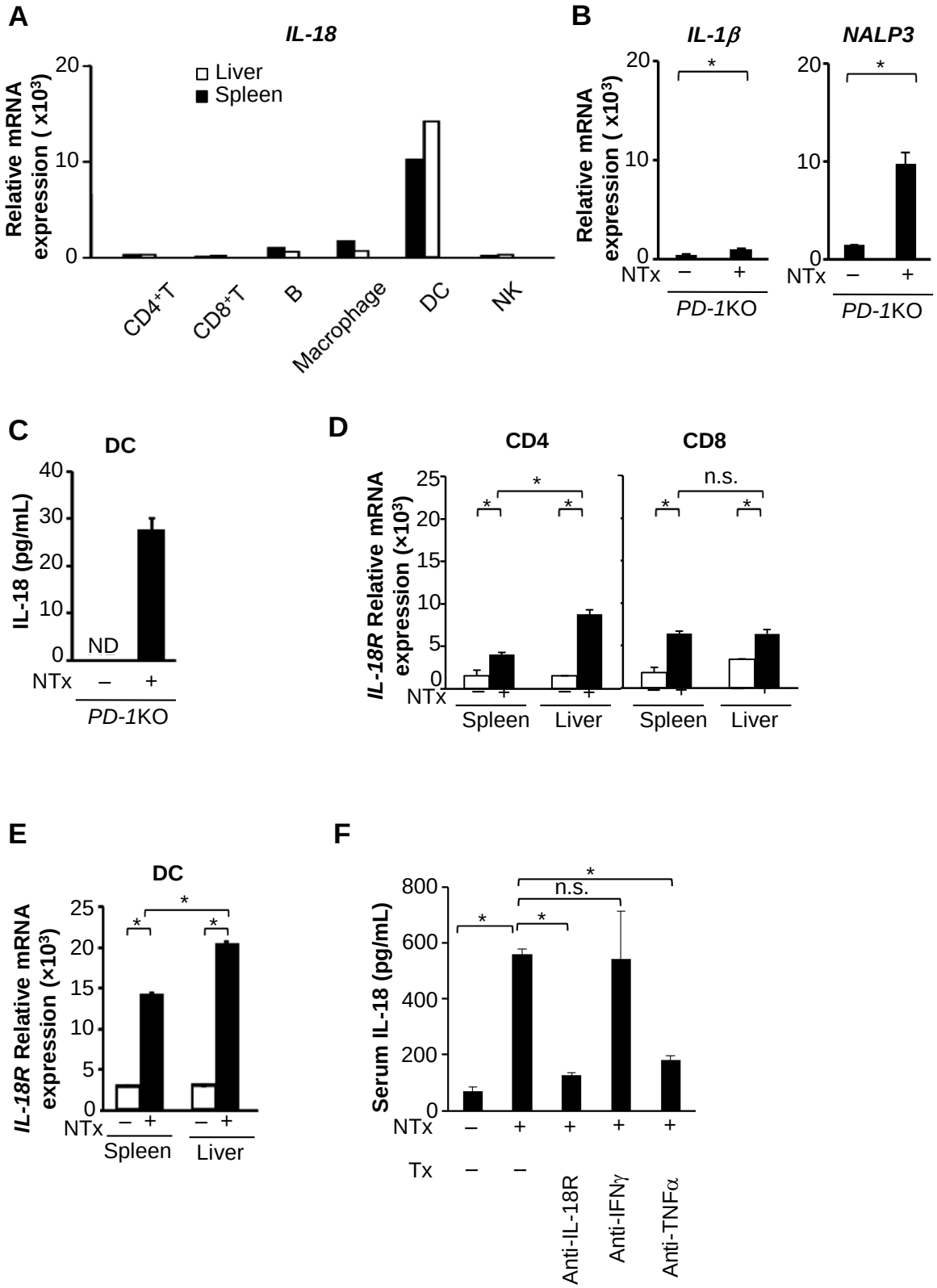
A
IL-18
Liver
Spleen
Relative mRNA expression (x10³)
20
10
0
CD4+T
CD8+T
B
Macrophage
DC
NK
B
IL-1β
NALP3
*
NTx – +
PD-1KO
C
DC
IL-18 (pg/mL)
40
30
20
10
0
ND
NTx – +
PD-1KO
D
CD4
CD8
IL-18R Relative mRNA expression (×10³)
25
20
15
10
5
0
n.s.
NTx
Spleen
Liver
Spleen
Liver
E
DC
IL-18R Relative mRNA expression (×10³)
NTx – + – +
Spleen
Liver
F
Serum IL-18 (pg/mL)
800
600
400
200
0
n.s.
NTx – + + + +
Tx – –
Anti-IL-18R
Anti-IFNγ
Anti-TNFα

Fig. 8.

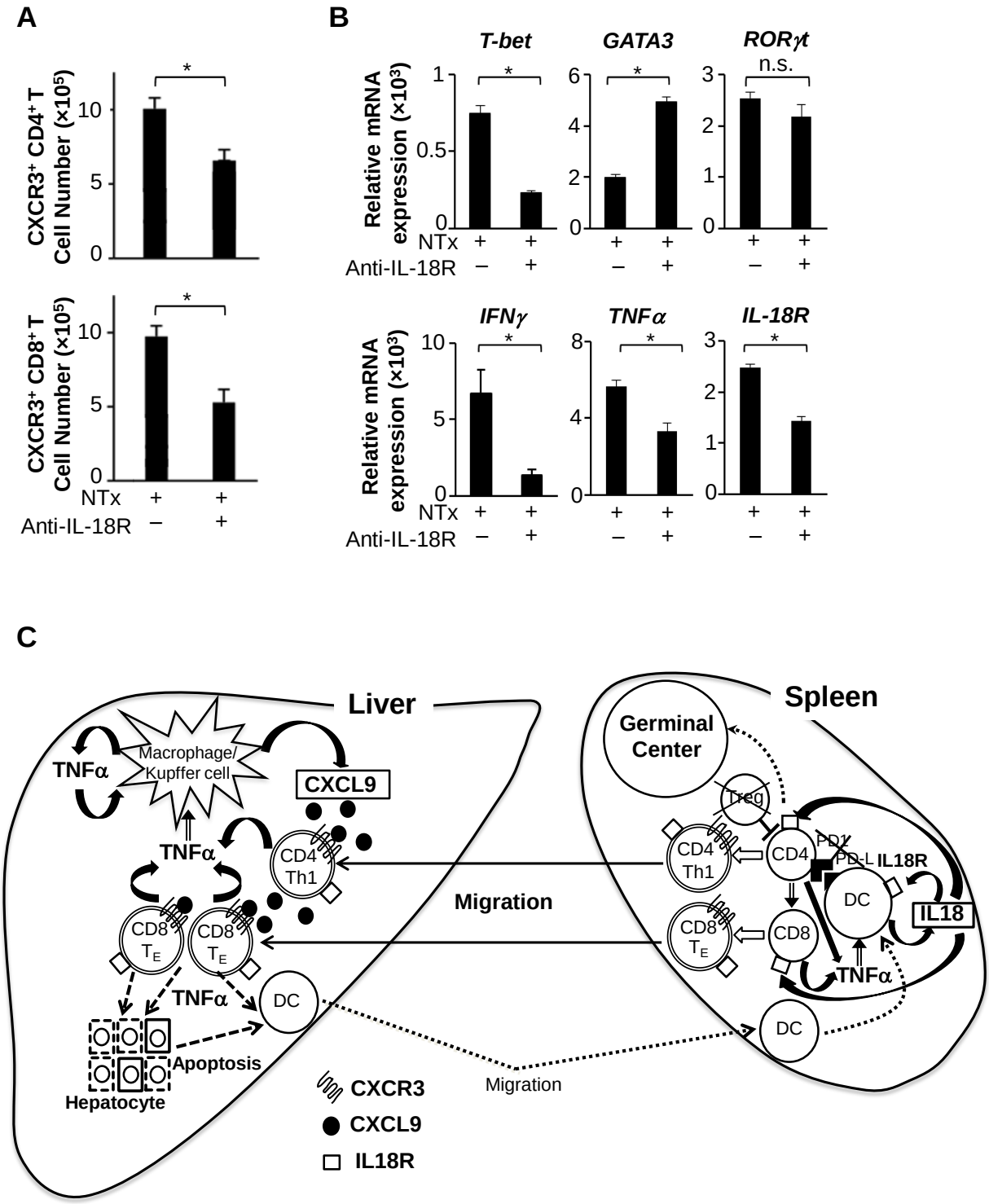
A
CXCR3+ CD4+ T Cell Number (×10^5)
CXCR3+ CD8+ T Cell Number (×10^5)
NTx
Anti-IL-18R
B
T-bet
GATA3
RORγt
n.s.
Relative mRNA expression (×10^3)
IFNγ
TNFα
IL-18R
C
Liver
Spleen
Macrophage/ Kupffer cell
TNFα
CXCL9
CD4 Th1
CD8 TE
Migration
DC
Apoptosis
Hepatocyte
Germinal Center
Treg
CD4
CD8
PD1
PD-L
IL18R
IL18
CXCR3
CXCL9
IL18R

<Supplementary Information>
Supplemental Materials and Methods

Histological and Immunohistological Analysis. Organs were fixed in neutral buffered formalin, embedded in paraffin wax, and cut into sections 4 μm thick. These sections were stained with hematoxylin and eosin for histopathology. Fluorescence immunohistology was performed on frozen sections using FITC-conjugated anti-CD4 or anti-CD8a (eBioscience, San Diego, CA), peanut agglutinin (PNA, Vector Laboratories, Burlingame, CA), biotin-labeled anti-B220 (BD Biosciences, San Jose, CA) followed by Texas red-conjugated avidin (Vector Laboratories) as described previously.[1-5] To stain CXCR3 ligands, rabbit polyclonal Abs to CXCL9/MIG (sc-50302, Santa Cruz Biotechnology, Santa Cruz, CA) and rat monoclonal Ab (mAb) to CXCL10/IP-10 (R&D Systems, Minneapolis, MN) were used, followed by Alexa Fluor 546 goat anti-rabbit IgG (Invitrogen, Carlsbad, CA) and FITC-conjugated goat anti-rat IgG (BD Biosciences), respectively. For staining of macrophages/kupffer cells, rat mAb to F4/80 (eBioscience) was used, followed by Alexa Fluor 488 goat anti-rat IgG (Invitrogen). As for the staining of TNFα, rabbit polyclonal Ab to TNFα (Abcam, Cambridge, UK) was used followed by Alexa Fluor 488 goat anti-rabbit IgG (Invitrogen). Germinal center (GC) diameters were measured in several high-power fields in at least three sections of each mouse, as described previously.[2]

Real-time Quantitative Reverse-transcription Polymerase Chain Reactions. (RT-PCR) Real-time quantitative RT-PCR was performed as described previously.[1-4] Spleen and liver tissues or isolated cells from the spleen and liver were frozen in RNAlater. RNA was prepared with an RNeasy mini kit (Qiagen, Hilden, Germany), and single-strand complementary DNA was synthesized with SuperScript™ II reverse transcriptase (Invitrogen). Real-time quantitative RT-PCR was performed using SYBR Green I Master (Roche Applied Science, Basel, Switzerland). The real-time quantitative reactions were performed using a Light Cycler 480 (Roche Applied Science) according to the manufacturer's instructions. Values are expressed as arbitrary units relative to glyceraldehyde-3-phosphate dehydrogenase (GAPDH). The following primers were used: *GAPDH*: 5'-CAACTTTGTCAAGCTCATTTCC-3' and 5'-GGTCCAGGGTTTCTTACTCC-3'; *T-bet*: 5'-TCAACCAGCACCAGACAGAG-3' and 5'-AAACATCCTGTAATGGCTTGTG-3';

GATA-3: 5’-TTATCAAGCCAAGCGAAG-3’ and 5’-TGGTGGTGGTCTGACAGTTC-3’;

ROR-γt: 5’-CCGCTGAGAGGGCTTCAC-3’ and 5’-TGCAGGAGTAGGCCACATTACA-3’;

IFN-γ: 5’-GGATGCATTCATGAGTATTGC-3’ and 5’-CCTTTTCCGCTTCCTGAGG-3’; *TNF-α*: 5’-CCCTCACACTCAGATCATCTTCT-3’ and 5’-GCTACGACGTGGGCTACAG-3’; *IL-1β:* 5’-TGTAATGAAAGACGGCACACC-3’ and 5’-TCTTCTTTGGGTATTGCTTGG-3’; *IL-4*: 5’-TCATCGGCATTTTGAACGAG-3’ and 5’-CGTTTGGCACATCCATCTCC-3’; *IL-13*: 5’-TGGGTGACTGCAGTCCTGGCT-3’ and 5’-GTTGCTTTGTGTAGCTGAGCA-3’; *IL-17A*: 5’-CTCCAGAAGGCCCTCAGACTAC-3’ and 5’-AGCTTTCCCTCCGCATTGACACAG-3’; *IL-18*: 5’-GACAACACGCTTTACTTTATACCTGA-3’ and 5’-GTGAAGTCGGCCAAAGTTGT-3’; *IL-18Rα*: 5’-GGAACACAACACGGACCAT-3’ and 5’-CGAGAAGGATGTATACAAACACCA-3’; *IL-22*: 5’-AGAAGGCTGAAGGAGACAGT-3’ and 5’-GACATAAACAGCAGGTCCAGTT-3’; *CXCR3:* 5’-GGCATCTAGCACTTGACGTTC-3’ and 5’-AGGCAGCACGAGACCTGA-3’*: CXCL9:* 5’-GCATCGTGCATTCCTTATCA-3’ and 5’-CTTTTCCTCTTGGGCATCAT-3’; *CXCL10:* 5’-TCTCACTGGCCCGTCATC-3’ and 5’-GCTGCCGTCATTTTCTGC-3’; *CXCL11:* 5’-CCCTGTTTGAACATAAGGAAGC-3’ and 5’-GCTGCTGAGATGAACAGGAA-3’; *NALP3*: 5’-TGCCTGTTCTTCCAGACTGGTGA-3’; 5’-CACAGCACCCTCATGCCCGG-3’.

Administration of Abs in vivo. NTx–*PD-1*$^{-/-}$ mice were intraperitoneally injected every week from day3 with 100μg of mAbs to CXCL9, CXCL10, IL-12p40 and IL1β (R&D Systems), IFNγ and TNFα (eBioscience), and IL-18Rβ (BD Bioscience), and from day17 with mAbs to TNFα. For depletion of $CD8^+$ T cells in vivo, anti-mouse CD8 mAbs (eBioscience) were used at day17 and day24. All isotypes were from

eBioscience or R&D Systems. After injections, mice at indicated ages were sacrificed, and their livers, spleens, and sera were harvested. We did not detect any serious adverse events.

Flow Cytometry Analysis and Isolation of Single Cells. Single cells from the livers and spleens were prepared, and flow cytometric analysis was performed as described previously.[1-5] Cells were stained with FITC-conjugated anti-CD3e (BD Bioscience), and either APC-Cy7-conjugated anti-CD4 (BD Bioscience) or APC-conjugated anti-CD8a (eBioscience). For chemokine receptors, cells were stained with FITC-conjugated anti-CD3e (145-2C11), APC-conjugated anti-CD8a (eBioscience), and PE-conjugated anti-CCR6, anti-CCR9 or anti-CXCR3 (R&D Systems). Stained cells were analyzed with FACSCanto™ II (BD Biosciences). Data were analyzed using Cell Quest Pro™ (BD Biosciences). Dead cells were excluded based on side- and forward-scatter characteristics. The number of viable indicated cells was calculated as follows: (the percentage of cells in the cell type) x (the number of viable cells). For isolation of cells in Figure 7A**,** the following mAbs were used for surface staining: FITC-conjugated anti-CD3e, anti-DX5, PE-conjugated anti-CD3e, anti-B220, APC-conjugated anti-CD8a, and PE-streptavidin purchased from eBioscience, FITC-conjugated anti-CD11c, biotinylated anti-CD11b, and APC-Cy7-conjugated anti-CD4 from BD Bioscience. $CD3^+CD4^+$, $CD3^+CD8^+$, $CD3^-B220^+$, $CD11b^+CD11c^-$, $CD11b^{+or-}CD11c^+$, $CD3^-DX5^+$ cells from the spleen or liver were obtained by a FACS Aria™ (BD Biosciences) to reach >99% purity, as described.[1,2] For $CD4^+$ T cell isolation in Figure 8B, NTx–*PD-1*$^{-/-}$ mice were injected intraperitoneally with anti-IL-18Rβ or isotype controls at one day after thymectomy and then once a week with the mAbs *in vivo*. After three mAbs injections, $CD4^+$ T cells were isolated from the spleens of three-week-old mice by positive selection using mouse CD4 microbeads (Miltenyi Biotec, Bergisch Gladbach, Germany) according to the manufacturer's instructions. $CD4^+$ T cells reached >94% purity, as assessed by flow cytometry.

Enzyme-Linked Immunosorbent Assay (ELISA). Concentrations of CXCL9 and CXCL10 in serum were measured by using mouse CXCL9 and CXCL10 ELISA kits (Abcam, Cambridge, UK) according to the manufacturer's protocols. To detect IL-18 in serum and culture supernatants, a mouse IL-18 ELISA kit (Medical & Biological

Laboratories, Nagoya, Japan) was used. Serum levels of IL-1β were measured using a mouse IL-1β ELISA kit (eBioscience). Serum Ig levels were determined by ELISA as described,[6] and Ab sets for detection of mouse IgG1 and IgG2a from BD Biosciences (San Jose, CA) and anti-mouse IgM from AbD Serotec (Oxford, UK) were used. To detect serum ANAs, microtiter plates (Nunc, Roskilde, Denmark) were incubated with 10 μg/ml antigens, and the nuclear fraction was prepared from normal liver.[7] Ab sets for detection of mouse ANA subclasses were the same as above.

In vivo Injection of Cytokines. *PD1*$^{-/-}$ mice at four weeks of age were injected intraperitoneally with 10μg/kg of mouse recombinant IFNγ, TNFα (eBioscience), or PBS. After 1, 2, 3, 6 or 9 hours following injections, mice were sacrificed, and their livers were harvested. We did not detect any serious adverse events.

Dendritic Cell (DC) Coculture. CD11b$^{+/-}$CD11c^{+} DCs were isolated from the spleen of 2.5-week-old NTx–*PD-1*$^{-/-}$ mice using a FACS Aria^{TM}II (BD Biosciences) to reach >99% purity, as described.[1,2] Isolated DCs (5×10^5) were cultured for 24 h in round-bottomed 96-well culture plates in D-MEM supplemented with 10% fetal bovine serum, 50 μmol/L 2-mercaptoethanol, 100 U/ml penicillin, and 100 μg/ml streptomycin.

Statistical Analysis. The data are presented as the mean values ± SD. Statistical analysis was performed by the Student's *t*-test for unpaired data to compare the values between two groups; variance was analyzed with the Tukey-Kramer test for multiple comparisons. Survival rates were estimated by the Kaplan-Meier method and compared with the log-rank test. *P*-values below .05 were considered significant.

References

1. Kido M, Watanabe N, Okazaki T, Akamatsu T, Tanaka J, Saga K, et al. Fatal autoimmune hepatitis induced by concurrent loss of naturally arising regulatory T cells and PD-1-mediated signaling. Gastroenterology 2008:135:1333-43.
2. Aoki N, Kido M, Iwamoto S, Nishiura H, Maruoka R, Tanaka J, et al. Dysregulated generation of follicular helper T cells in the spleen triggers fatal autoimmune hepatitis in mice. Gastroenterology 2011;140:1322-33.
3. Iwamoto S, Kido M, Aoki N, Nishiura H, Maruoka R, Ikeda A, et al. IFN-γ is reciprocally involved in the concurrent development of organ-specific autoimmunity in the liver and stomach. Autoimmunity 2012;45:186-98.
4. Iwamoto S, Kido M, Aoki N, Nishiura H, Maruoka R, Ikeda A, et al. TNF-α is essential in the induction of fatal autoimmune hepatitis in mice through upregulation of hepatic CCL20 expression. Clin Immunol. 2013;146(1):15-25.
5. Maruoka R, Aoki N, Kido M, Iwamoto S, Nishiura H, Ikeda A, et al. Splenectomy prolongs the effects of corticosteroids in mouse models of autoimmune hepatitis. Gastroenterology. 2013;145:209-220.
6. Muramatsu M, Kinoshita K, Fagarasan S, Yamada S, Shinkai Y, Honjo T. Class switch recombination and hypermutation require activation-induced cytidine deaminase (AID), a potential RNA editing enzyme. Cell 2000;102:553-63.
7. Blobel G, Potter VR. Nuclei from rat liver: isolation method that combines purity with high yield. Science 1966;154:1662-5.

Supplementary Fig. 1.

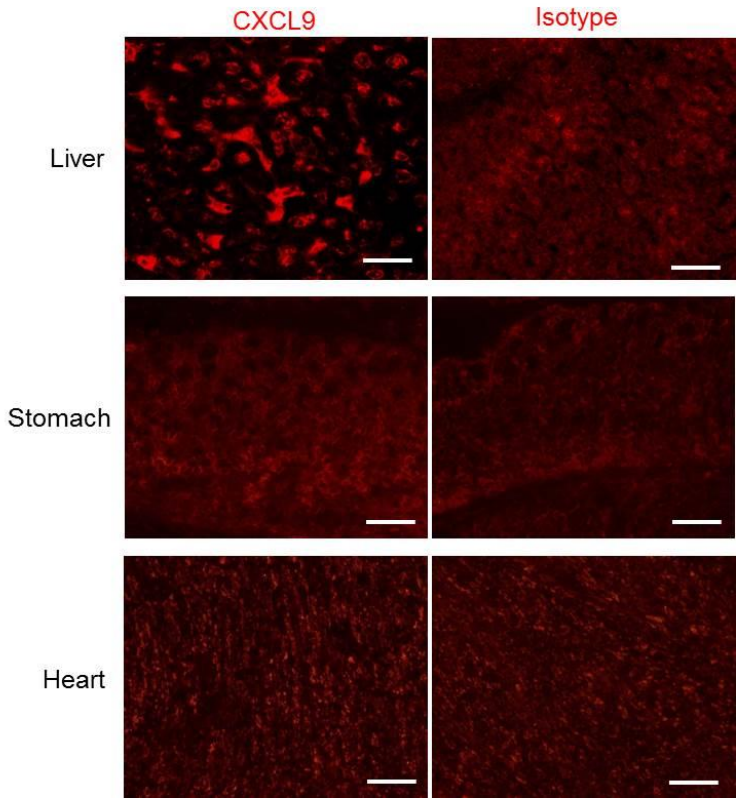

Supplementary Fig. 1. Immunohistological analysis of the liver, stomach and heart in NTx–*PD-1*$^{-/-}$ mice. Immunostaining with anti-CXCL9 or isotype control. The livers from three-week-old NTx–*PD-1*$^{-/-}$ mice were used. Scale bars, 50 μm.

Supplementary Fig. 2.

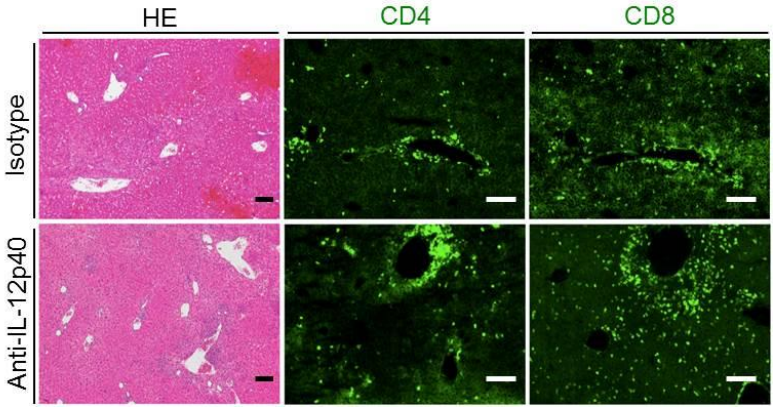

Supplementary Fig 2. Histological and immunohistological analysis for the liver in NTx–*PD-1*$^{-/-}$ mice injected with neutralizing Abs for IL-12p40. (A) NTx–*PD-1*$^{-/-}$ mice at one day after thymectomy were injected intraperitoneally every week with 100 μg of neutralizing anti-IL-12p40 (n=5) or the isotype control mAb (n=5). After four injections, mice at four weeks of age were sacrificed, and the livers were harvested. Representative stainings of the liver for hematoxylin and eosin (HE), CD4, and CD8 are shown. All *scale bars*, 100 μm.

Supplementary Fig. 3.

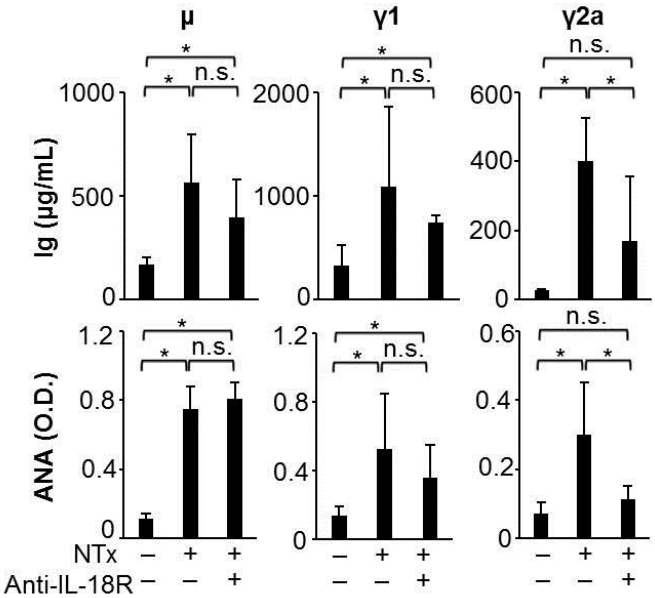

Supplementary Fig. 3. Immunological analysis for NTx–*PD-1*$^{-/-}$ mice injected with blocking Abs for IL-18R signaling. NTx–*PD-1*$^{-/-}$ mice at one day after thymectomy were injected intraperitoneally every week with 100 μg of IL-18Rβ mAb (n=10), or the isotype control mAb (n=10). After four injections, mice at four weeks of age were sacrificed. The serum levels of total immunoglobulin (Ig) and ANAs subclasses in IgM, IgG1, and IgG2a in indicated mice were determined by ELISA. *Error bars* represent SD. *Asterisks* indicate $P < 0.05$. n.s., not significant.

Supplementary Fig. 4.

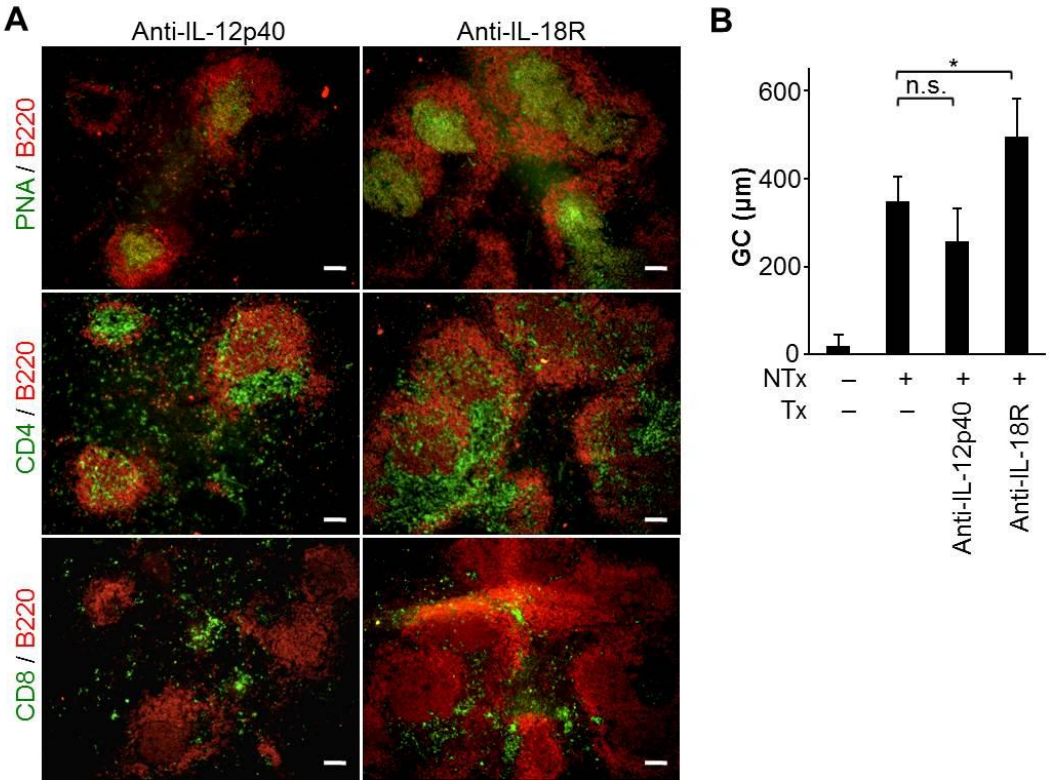

Supplementary Fig. 4. Immunohistological analysis for NTx–*PD-1*$^{-/-}$ mice injected with blocking Abs for IL-18R signaling and with neutralizing Abs for IL-12p40. NTx–*PD-1*$^{-/-}$ mice at one day after thymectomy were injected with anti-IL-12p40 or IL-18Rβ mAb. After four injections, mice at four weeks of age were sacrificed as described in Supplementary Fig. 2 and Fig. 3. Immunohistological analysis of the spleens from mice with indicated treatments (A) and diameters of germinal center (GC) in the follicles of the spleen. Spleens were stained with FITC-conjugated anti-CD4, anti-CD8, or PNA (green) and biotin-labeled anti-B220 followed by Texas red-conjugated avidin (red). Diameters of PNA^{+} GC in the B220^{+} follicles were determined in several high-power fields. Data are shown as the mean of at least three mice. *Error bars* represent SD. *Asterisks* indicate $P < 0.05$. n.s., not significant. Scale bars, 100 μm.